

Review

Photophysics and Photochemistry of Iron Carbene Complexes for Solar Energy Conversion and Photocatalysis

Linnea Lindh ^{1,2}, Pavel Chábera ¹, Nils W. Rosemann ¹, Jens Uhlig ¹,
Kenneth Wärnmark ³, Arkady Yartsev ¹, Villy Sundström ^{1,*} and Petter Persson ^{2,*}

¹ Division of Chemical Physics, Department of Chemistry, Lund University, Box 118, SE-22100 Lund, Sweden; linnea.lindh@chemphys.lu.se (L.L.); Pavel.Chabera@chemphys.lu.se (P.C.); nils.rosemann@chem.lu.se (N.W.R.); jens.uhlig@chemphys.lu.se (J.U.); arkady.yartsev@chemphys.lu.se (A.Y.)

² Theoretical Chemistry Division, Chemistry Department, Lund University, Box 118, SE-22100 Lund, Sweden

³ Center for Analysis and Synthesis, Department of Chemistry, Lund University, Box 118, SE-22100 Lund, Sweden; Kenneth.Warnmark@chem.lu.se

* Correspondence: Villy.Sundstrom@chemphys.lu.se (V.S.); Petter.Persson@teokem.lu.se (P.P.)

Received: 29 January 2020; Accepted: 5 March 2020; Published: 10 March 2020



Abstract: Earth-abundant first row transition metal complexes are important for the development of large-scale photocatalytic and solar energy conversion applications. Coordination compounds based on iron are especially interesting, as iron is the most common transition metal element in the Earth's crust. Unfortunately, iron-polypyridyl and related traditional iron-based complexes generally suffer from poor excited state properties, including short excited-state lifetimes, that make them unsuitable for most light-driven applications. Iron carbene complexes have emerged in the last decade as a new class of coordination compounds with significantly improved photophysical and photochemical properties, that make them attractive candidates for a range of light-driven applications. Specific aspects of the photophysics and photochemistry of these iron carbenes discussed here include long-lived excited state lifetimes of charge transfer excited states, capabilities to act as photosensitizers in solar energy conversion applications like dye-sensitized solar cells, as well as recent demonstrations of promising progress towards driving photoredox and photocatalytic processes. Complementary advances towards photofunctional systems with both Fe(II) complexes featuring metal-to-ligand charge transfer excited states, and Fe(III) complexes displaying ligand-to-metal charge transfer excited states are discussed. Finally, we outline emerging opportunities to utilize the improved photochemical properties of iron carbenes and related complexes for photovoltaic, photoelectrochemical and photocatalytic applications.

Keywords: iron; *N*-heterocyclic carbene (NHC); photophysics; photochemistry; photocatalysis; solar energy conversion; dye-sensitized solar cells; artificial photosynthesis; solar fuels

1. Introduction

Earth-abundant transition metal complexes have received growing attention in the last decade, offering appealing opportunities to develop sustainable large-scale molecular-based technologies in the closely related fields of solar energy conversion and photocatalysis [1–6]. Complexes are sought to provide favorable photoredox-properties rivalling or exceeding the photophysical and photochemical properties of the best current transition metal complexes, but using only non-toxic and environmentally friendly metals that would be widely available for large-scale applications at competitive costs. Finding Earth-abundant alternatives to photofunctional transition metal complexes currently based on heavy and rare elements such as ruthenium, iridium, and platinum does, however, offer significant challenges.

On one hand, the most abundant transition metal elements all belong to the first transition metal row, with iron being the most common transition metal element of all in the Earth's crust (Figure 1). With iron situated among the group 8 elements together with ruthenium and osmium that have favorable electronic configurations (d^6 in octahedral complexes for the metal ions in oxidation state II), it should be well positioned to be a prominent candidate for large-scale photochemical applications, as realized early on e.g., in the field of solar energy [7–14]. However, the photophysics and photochemistry of transition metal complexes largely depend on the ability to utilize ligands to influence the key valence d-level electrons of the transition metals that are involved in excited states and photochemical reactions, but these are much more difficult to influence in first row transition metal complexes, due to the 3d-levels being less accessible. This is known as the primogenic effect and can be traced back to the small atomic orbital radius of the 3d level relative to those of the 4s and 4p valence levels, for the first row transition metals as recently highlighted by McCusker [15]. Thus, while iron in some senses is the most appealing of all transition metal elements from an industrial, sustainable and eco-friendly perspective, it is at the same time among the scientifically most challenging elements to make work for photochemical applications.

As a brief summary of earlier work on photoexcited iron complexes, it is worth recalling that the photophysics of transition metal complexes based on iron has been widely investigated as a prototype case for (quasi-)octahedral d^6 first row transition metal complexes, see, e.g., [16,17]. Rather than displaying long-lived metal-to-ligand charge transfer (MLCT) states with high excited state energy that has promoted the widespread use of Ru(II) polypyridyl photosensitizers, photoexcited iron complexes typically undergo ultrafast deactivation to high-spin metal centered (MC), sometimes also referred to as ligand field (LF), states. This has provided a rich field for investigating ultrafast deactivation dynamics in prototype Fe(II) and Fe(III) polypyridyl and cyanometallate complexes, often involving a cascade of excited state dynamics including photoexcitation, intersystem crossing (ISC), and initiation of structural relaxation on ultrafast timescales. In particular, sub-ps spin-crossover and ultrafast deactivation from initially excited charge transfer (CT) states to intermediate-(triplet) and high-spin (quintet) metal centered states have been studied in detail experimentally [18–20], as well as theoretically [21]. Related topics that have been of particular interest include excited state dynamics in dye-sensitized solar cells (DSSCs) with iron-based light-harvesters [22], light-induced relaxation dynamics in Fe(III) complexes [23], and the role of spin-vibronic mechanisms on intersystem crossing [24]. The great difference in photophysics, and particularly the characteristic ultrafast deactivation compared to corresponding Ru complexes, is mainly associated with the much weaker ligand field splitting that is reflected in a smaller destabilization of the e_g -levels on the metal center in Fe compared to Ru [25]. This makes the metal centered states in which the e_g levels are populated much more accessible from initially populated CT states in complexes based on iron compared to ruthenium. The underlying electronic structure properties associated with this, as well as the remedial effects provided by the *N*-heterocyclic carbene (NHC) ligands in terms of strong σ -donation, etc., are discussed in more detail in Section 2 of this review. In particular, current progress with both Fe(II) and Fe(III)NHC complexes warrants an exposition of the balance between CT and MC states in the two fundamentally distinct electronic structure cases.

Rapid progress towards functioning iron carbene photosensitizers commencing in 2013 has been manifested in a growing number of important investigations of different photophysical and photochemical properties as the subject of this review. Selected developments that are discussed in this review are charted on a timeline in Figure 2.

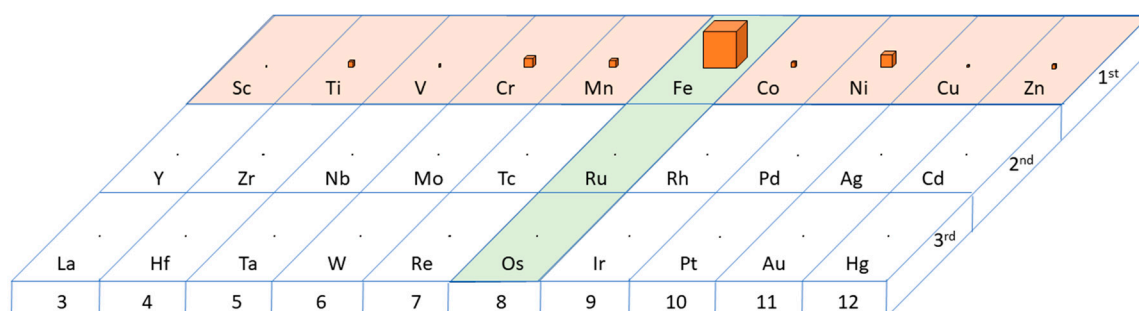


Figure 1. Relative atomic abundances of transition metal elements, highlighting the importance of the first row transition metal element iron (Fe), in terms of its combination of highest natural abundance of all transition metal atoms, as well as its belonging to the photochemically favorable group 8 together with rare ruthenium (Ru) and osmium (Os). Relative atomic abundances in the Earth's crust according to data from Ref. [26] are proportional to the volumes of the cubes.

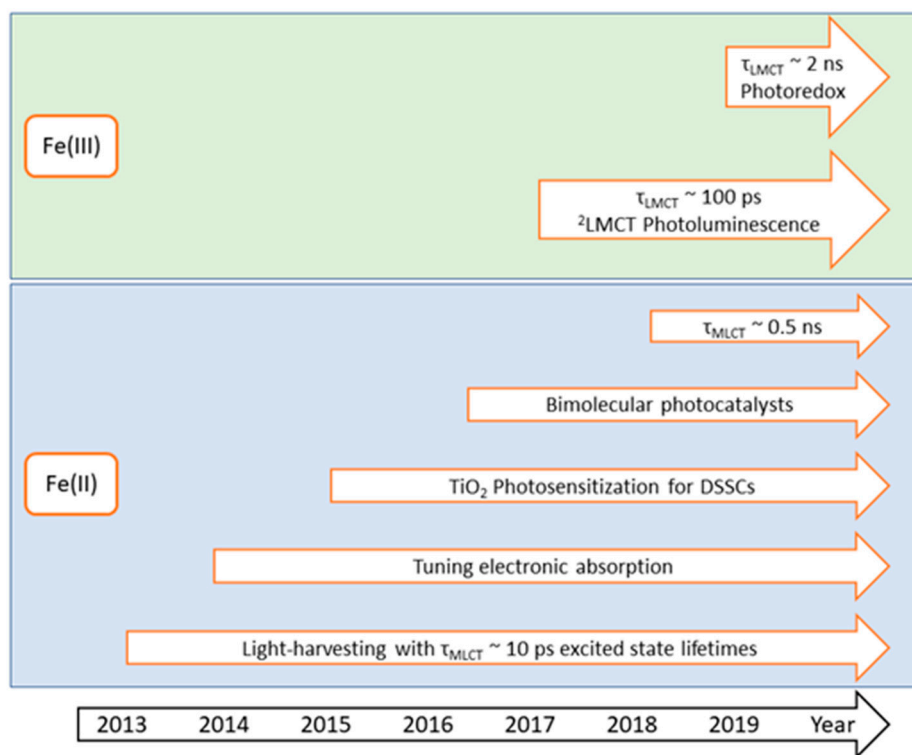


Figure 2. Timeline highlighting selected key developments for Fe(II) and Fe(III) *N*-heterocyclic carbene NHC complexes discussed in the text.

In part driven by the rapid progress for iron-based photosensitizers, and in part due to a generally growing interest in photofunctional Earth-abundant transition metal complexes, different aspects of this subject matter have also been covered in some recent reviews. While an account of the broader research field goes beyond the present scope, it is pertinent to briefly list key reports directly addressing iron *N*-heterocyclic carbene (NHC) complexes here, as a guide to the reader of where to find additional overview information. A first account of early progress towards iron carbene photosensitizers from the perspective of the collaborative iron carbene group in Lund was presented by Liu et al. in 2016 [9]. This account outlined several paths towards Fe(II) photosensitizers with long-lived triplet metal-to-ligand charge transfer (3MLCT) excited states and included work up to the demonstration of sensitization of nano-TiO₂ leading to efficient interfacial charge transfer, reported in 2016. Abrahamsson furthermore included iron carbene complexes in the context of iron polypyridyl-type complexes for solar energy

applications in a review-style book chapter [10]. Wenger highlighted several findings from the work on iron carbenes in broader reviews dedicated to emerging Earth-abundant light-harvesting transition metal complexes, providing a valuable comparative analysis of different kinds of emerging first-row photoactive transition metal complexes, including, e.g., isoelectronic Cr(0)isocyanide analogues from their own work [3]. In a recent perspective, he furthermore poignantly asked if the progress with iron-based photosensitizers is sufficient to consider iron as the new ruthenium [11]. Some ultrafast photophysical aspects of both Fe(II) and some of the first promising results for Fe(III) were included in a broader context about ultrafast electron dynamics for solar energy conversion [27]. Chen and Brown recently wrote about the photochemistry of iron complexes [28], and Vöhringer also included FeNHC complexes in a review with a focus on time-resolved investigations about the initial steps in homogeneous catalysis [29]. Progress on FeNHC photosensitizers were included in a review by Elliott and co-workers discussing the photophysics and photochemistry of a wider range of metal complexes, specifically employing triazole ligands [30]. The particular topic of using iron NHC complexes for dye-sensitized solar cell (DSSC) applications has also been recently covered [31]. Pastore et al. also recently presented a broad computational perspective on excited state properties, including work on iron carbenes [32]. Finally, we have recently written an in-depth account focusing on photofunctional d^5 complexes, where the iron(III) carbene complexes are placed in context of earlier photochemical work on iron(III) and other d^5 complexes, notably including some Re(II) third-row transition metal complexes [33].

Our ambition here is to provide a concise review of key progress regarding the photophysical and photochemical properties of iron carbene complexes from 2013 and up to and including 2019. Given the rapid development of this research area, the ambition here has been to include a comprehensive survey of key developments without unduly repeating lengthy discussions from previous reviews mentioned for some of the early work, which is referenced when beneficial. This review is also accompanied in this issue by a review by Kaufhold and Wärnmark focused on the design and synthesis of the iron carbenes [34].

2. Photophysics of FeNHC Complexes

Due to its high natural abundance, there has been a long-standing interest to develop iron-based photosensitizers and photocatalysts, reaching back at least fifty years. This particularly includes an interest to develop materials for solar energy conversion, in terms of both molecular photovoltaics and artificial photosynthesis or solar fuels [1]. From a fundamental photophysical perspective, Fe(II) complexes feature a similar d^6 electronic configuration with large t_{2g} - e_g splitting in octahedral (or quasi-octahedral) hexa-coordinated complexes. This has allowed the successful development of innumerable complexes based on Ru(II) as the second-row transition metal congener from group 8 [7,8]. Briefly, these Ru(II) complexes typically feature visible absorption from a singlet ground state (1GS) to excited singlet metal-to-ligand charge transfer (1MLCT) states. This subsequently converts by intersystem crossing into long-lived (typically 100's of ns to μs) triplet MLCT (3MLCT) excited states with sufficiently high excited state energies (typically ~ 2 eV), to drive many photochemical applications [8,27,35,36].

Many corresponding iron(II) complexes, such as $[Fe^{II}(bpy)_3]^{2+}$ (bpy is 2,2'-bipyridine), have similar MLCT absorption capabilities as the Ru(II) complexes, but instead of remaining in the high-energy 3MLCT state they decay on ultrafast timescales through ISC into low-energy high-spin (quintet) metal centered states (5MC), sometimes alternatively referred to as ligand field (LF) states [14,16,17,37–39]. This issue is particularly pronounced given the intrinsically smaller ligand field splitting of the t_{2g} - e_g levels in first row transition metal complexes, compared to heavier congeners from the second and third transition metal rows [15].

A prototype electronic structure scheme, including the most important metal (M) and ligand (L) frontier levels and their interactions, is shown in Figure 3a. Figure 3b furthermore highlights the specific metal–ligand orbital interactions involving the carbene ligands. A corresponding state

perspective is shown in Figure 3c, including the key ground and excited state potential energy landscape. An interesting common feature of low-spin (LS) to high-spin (HS) transitions is that population of e_g -levels in the HS case typically drive an expansion of M–L bond lengths by ca 0.2 Å or more (~10% expansion for relevant Ru–L and Fe–L bond lengths of ca 2 Å). Notably the deactivation cascade includes a transition from $(e_g)^0$ in the LS case, via $(e_g)^1$ in the intermediate spin (IS) 3MC case, to $(e_g)^2$ in the HS case. With the electronic transitions coupling strongly to significant structural changes involving several M–L bonds, and furthermore potentially including Jahn–Teller degeneracies (particularly for the 3MC state), in high-symmetry systems this provides for an interesting case of rich and multi-dimensional ultrafast dynamics. Such light-induced excited spin-state trapping (LIESST) processes of meta-stable high-spin states, as well as closely related spin crossover (SCO) properties, may be interesting for molecular opto-magnetic applications [40–42]. However, the significant energy losses associated with transitions into the MC states has largely curtailed the usefulness of these complexes for light-harvesting or light-emitting applications [9,10,15,17]. Several theoretical studies have also been presented for different spin and/or oxidation states, including exploration of the potential energy landscapes of FeNHC and other Fe complexes with different M–L interactions. These studies cover key aspects of the energy balance between key states in the deactivation cascades, including elucidation of different strategies to characterize and ultimately influence the relative energies of CT and high/intermediate/low spin MC states, as well as structural relaxations/distortions in the states involved in the excited state cascade [17,21,27,43–50].

Recent progress to promote long-lived CT states in Fe(II)NHC complexes discussed in this review largely relies on the exceptionally strong σ -donating capabilities of the carbene-based ligands (Figure 3), that have strongly contributed to their usefulness in the field of homogeneous catalysis [51]. This σ -donation has a pronounced effect on the photophysics of the FeNHC complexes as the MC states are destabilized, significantly altering the accessibility of the MC states from the MLCT states as illustrated in Figure 3b. For a given CT excited state energy, sufficient raising of the MC potential energy surfaces can introduce an energy barrier to CT→MC conversion that can significantly slow down the decay into these scavenger MC states, even if the relaxed MC states are lower in energy than the relaxed 3MLCT energy (again illustrated in Figure 3c).

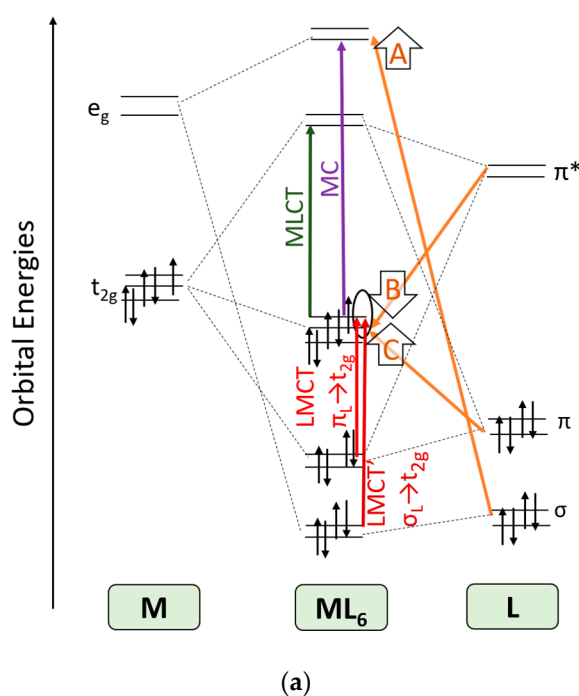


Figure 3. Cont.

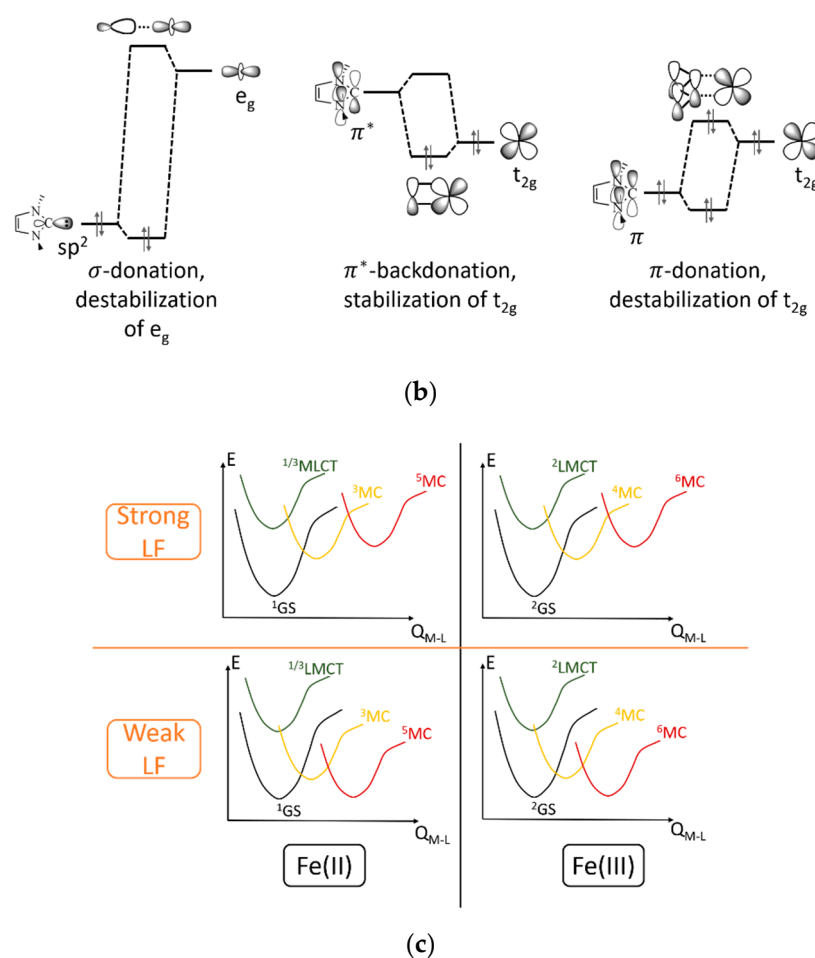


Figure 3. Schematic illustration of electronic structure of quasi-octahedral Fe(II) and Fe(III) NHC complexes. (a) Prototype metal-ligand bonding interactions and typical optical excitations in FeNHC complexes. Note that the ligand-to-metal charge transfer (LMCT) excitations to the t_{2g} levels are generally absent in Fe(II) complexes with a filled (t_{2g})⁶ configuration on the metal center. (b) carbene-metal donation and backdonation interactions (illustrated under the assumption of a (t_{2g})⁶ electronic configuration for a Fe(II) complex). (c) Fe(II) and Fe(III) prototype ground and excited state potential energy schemes in weak and strong ligand field environments.

Interestingly, a similar change in relative energies between CT and MC states with increased destabilization of the e_g -levels can be seen also for the d^5 case of Fe(III), for the yet more surprising recent advancement of photofunctional Fe(III)NHC complexes featuring long-lived low-spin (doublet) ligand-to-metal CT (2LMCT) states [52,53]. Recent progress in the understanding of photophysical origins, as well as current photochemical capabilities and emerging opportunities for solar energy conversion and photocatalytic applications for this unconventional $d^5/Fe(III)$ motif are discussed further in Section 4.

3. Fe(II)NHC Complexes

3.1. Homoleptic $Fe^{II}(CNC)_2$ Complexes

Initial progress towards better photophysical properties of iron(II) complexes with NHC ligands was first reported in 2013 by Liu et al. [54], utilizing the novel synthesis of complexes **1** and **2** (chemical structures shown in Figure 4 together with the chemical structures of iron NHC complexes **1–30** discussed in this paper), in an investigation carried out together with complementary quantum chemical calculations by Fredin et al., reported separately [44].

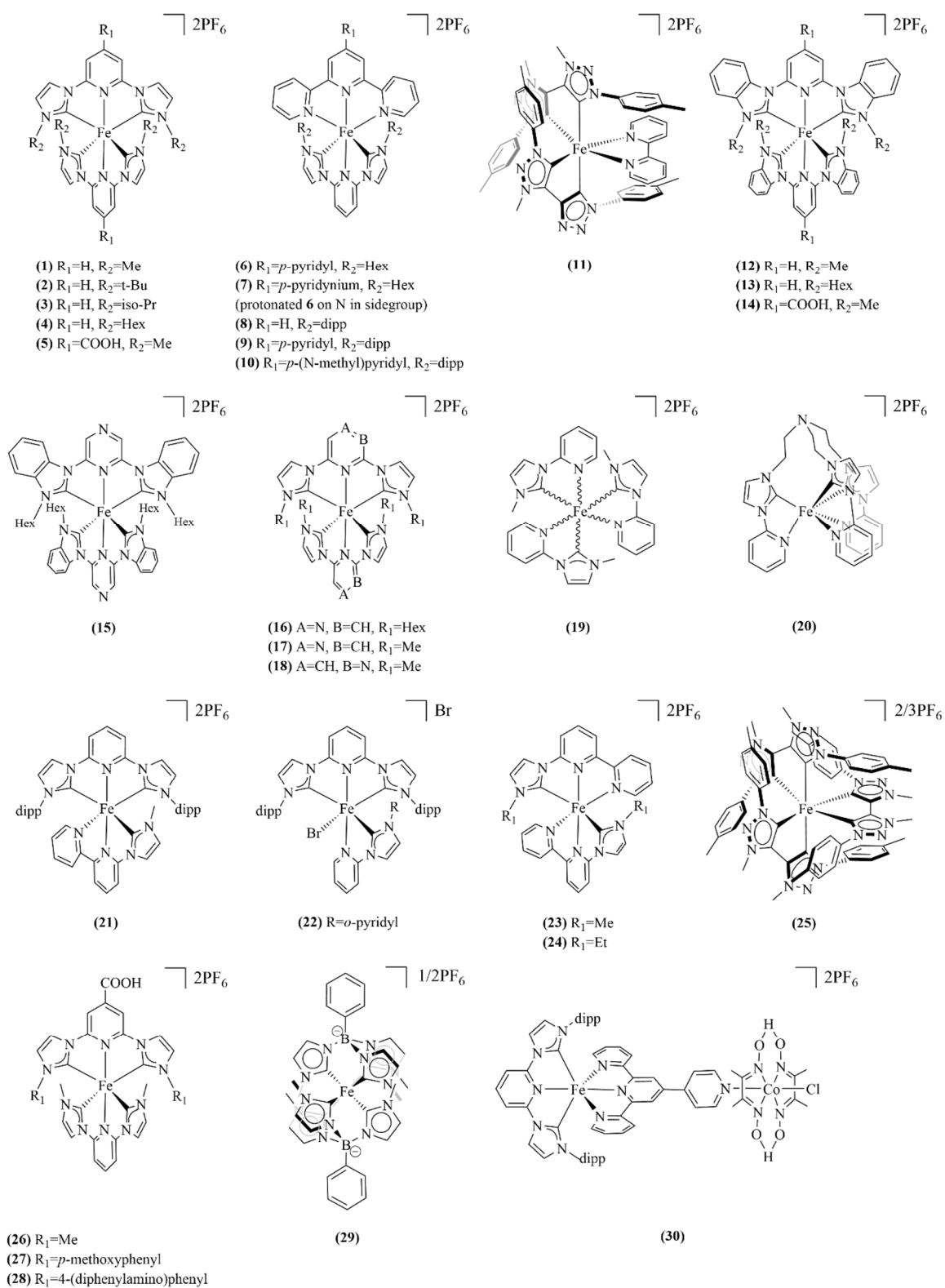


Figure 4. Chemical structures of photofunctional FeNHC complexes discussed in the text; dipp=diisopropylphenyl.

The UV/VIS absorption spectrum of complex **1** displaying the strongest MLCT peak at 457 nm is shown in Figure 5, together with corresponding absorption spectra of several FeNHC complexes discussed in subsequent sections.

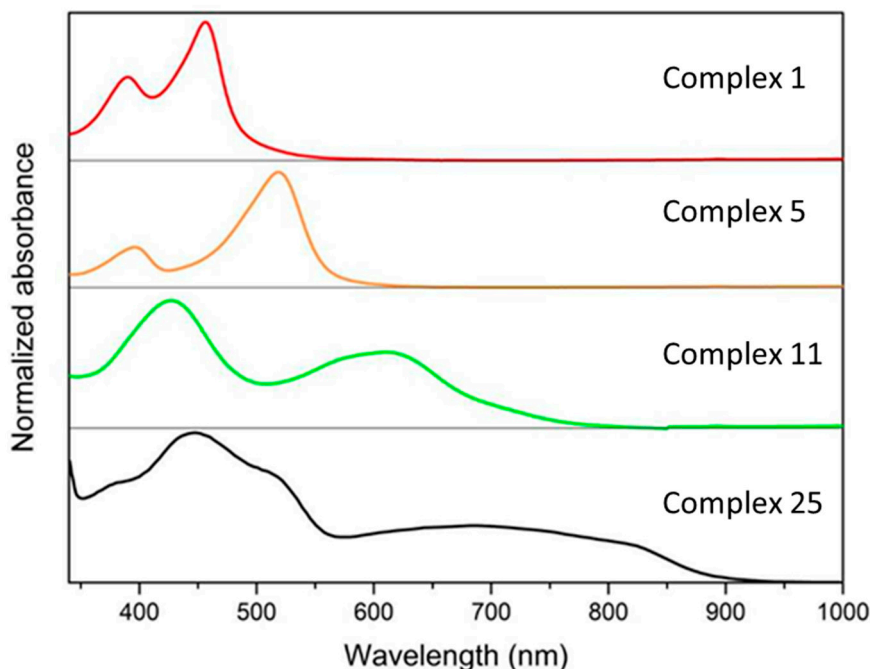


Figure 5. Steady-state absorption spectra of Fe(II) complexes **1**, **5**, **11**, and **25** in dry acetonitrile, illustrating a gradual extension of the low energy absorption bands towards the red part of the visible spectrum with different carbene modifications discussed in the text. All spectra are normalized and vertically offset for clarity.

Instead of ultrafast deactivation from initially excited MLCT states to meta-stable high-spin (quintet) metal centered states (5MC) occurring on sub-picosecond (sub-ps) timescales in typical iron polypyridyl complexes, complex **1** displayed a markedly extended excited state lifetime of 9 ps (Table 1 and Figure 6). This was assigned to the lifetime of the 3MLCT state using a combination of experimental photo(electro)chemical information together with complementary quantum chemical calculations. Moreover, the 9 ps excited state lifetime of complex **1** was mirrored by a similar lifetime for ground state recovery (Figure 6a). This deactivation behaviour is in stark contrast to typical lifetimes of 100s' of ps or longer for meta-stable 5MC scavenger states seen in e.g., $[Fe^{II}(tpy)_2]^{2+}$ used as a reference bis-tridentate complex and in complex **2** (Figure 7), whose bulkier tert-butyl side-groups provided steric hindrance blocking ideal metal coordination. Together these contrasting findings of the photocycles of complexes **1** and **2** provided early evidence that the strong σ -donating capabilities of the NHC ligands indeed put these complexes in a promising position for further improvements of the excited state lifetimes.

Table 1. Photo(electro)chemical properties of Fe(II)NHC complexes. All measurements in CH₃CN and with PF₆ counterions unless otherwise noted. Electrochemical measurements conducted in CH₃CN against Fc⁺⁰ and converted to corresponding standard NHE values using a standard reference electrode conversion constant of +0.630 V [55].

Complex	$\lambda_{\text{absmax}}^a$ /nm	ϵ /M ⁻¹ cm ⁻¹	$\tau_{\text{MCLT}}/\text{ps}$	$E_{1/2}(\text{Fe}^{\text{III/II}})$ /V vs. NHE	$E_{1/2}(\text{L}^{-/0})^b$ /V vs. NHE	Ref
1	457	15200	9	0.94	-1.76	[54]
2	478	14800	0.3	1.03	-1.72	[54]
3	458 ^c	14500 ^c	8.1	1.06	-1.68 ^d	[56,57]
4	460	15900	12	1.04	-1.71 ^d	[31,58]
5	520	16200	16.5	1.09	-1.11 ^d	[59]
6	522 (560)	9500	2.7 ^e	1.17	-1.18	[31,58]
7	590	11500	-	1.19	-1.02	[58]
8	503 (538) ((630)) ^c	9800 ^c	< 0.1	1.19	-1.26	[57,60]
9	515 (553) ((630))	10000	1.1	1.23	-1.13	[56]
10	586	12700	-	1.29	-0.56	[56]
11	432 (609) ((720))	5100	13	0.28	-1.65 ^d	[61]
12	440	12500	16.4	1.28	-1.56 ^d	[62]
13	445	-	19.5	-	-	[31]
14	501	12800	26	1.37	-0.99 ^d	[62]
15	479	16200	32 ^f	1.46	-0.97	[63]
16	493	17300	22 ^f	1.33	-1.08	[63]
17	487	16100	23 ^f	1.22	-1.15	[63]
18	477	12600	12 ^f	1.17	-1.46 ^d	[63]
19	430	12000	g	0.89	-1.73 ^d	[64,65]
20	438	8000	g	0.85	-1.70 ^d	[65]
21	409 (466, 506, 538)	6400	3.6	1.09	-1.30	[60]
22	-	-	-	-	-	[60]
23	557 ((640))	7000	<0.1	1.07	-1.11	[60]
24	560 ((620))	6000	0.12	1.08	-1.11	[31]
25	440 (510, 690, 825)	5600	528	0.05	-1.75	[66]
26	506	12700	14	1.06	-1.11 ^d	[32]
27	509	17700	10	1.05	-1.09 ^d	[32]
28	509	9500	12	1.06	-1.10 ^d	[32]
30	379 (520, 558) ((630))	10300	1.4	1.26	-0.27 ^{d,h}	[56]

^a Most intense peak in MLCT band. Reported significant peaks at lower excitation energies are given in parenthesis, very low intensity peaks/shoulders in double parenthesis. ^b Only first reduction potential, assumed to be ligand based unless otherwise noted. ^c Measured with BPh₄ as counterion. ^d Reported as irreversible reduction. ^e Uncertain nature of the excited state. ^f Listed lifetime reflects the effective average lifetime of an equilibrium of ³MLCT and ³MC states according to model in ref [63]. ^g Depending on fac- or mer-isomer. Excited state modelled as an equilibrium of ³MLCT and ³MC states, see ref [65] for more information. ^h Reduced species unstable under the measurement conditions, ligand reduction character not confirmed.

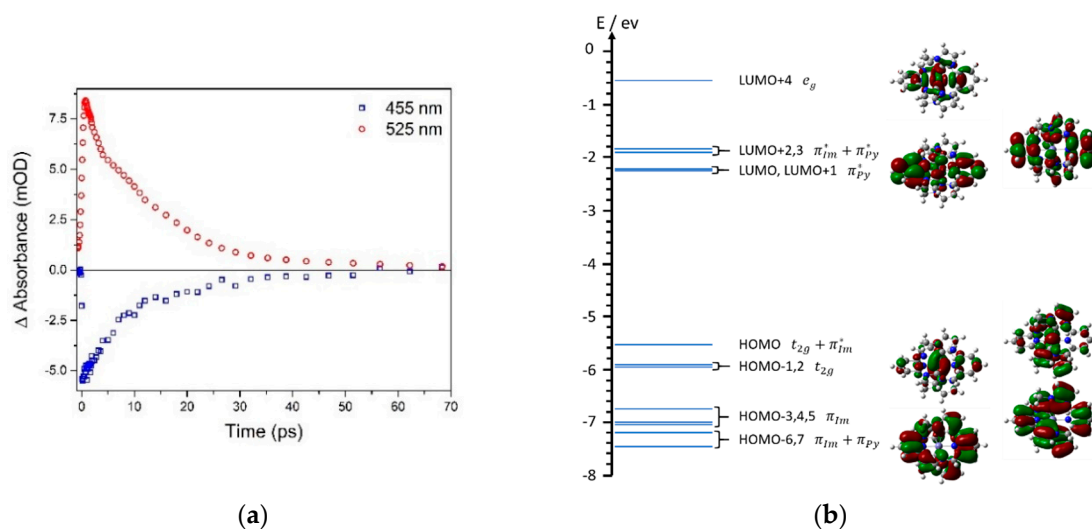


Figure 6. Cont.

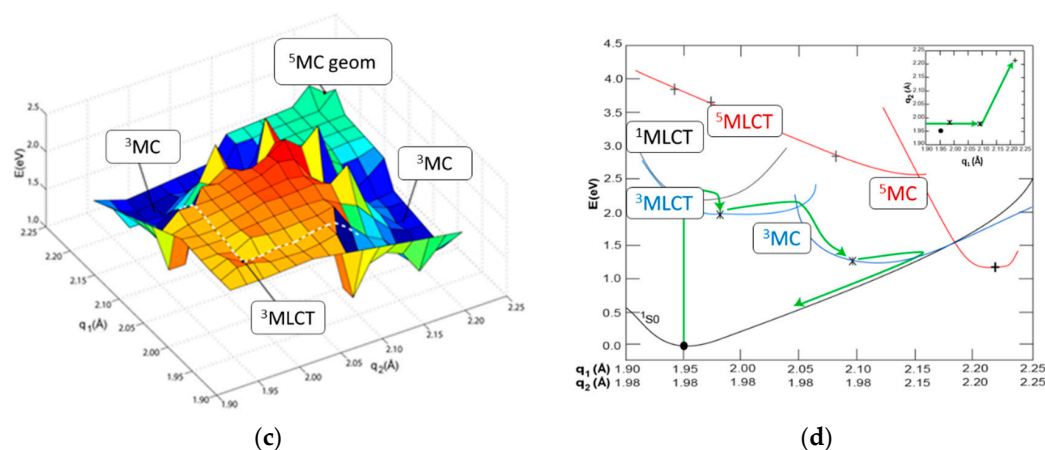


Figure 6. Photophysics of complex **1**. (a) Transient absorption kinetics of complex **1** following 480 nm excitation, recorded at 455 nm (blue squares) in the ground-state bleach region and at 525 nm (red circles) at the excited state absorption maximum. (b) molecular orbital diagram with selected Kohn-Sham (KS) orbitals displayed from B3LYP*/6-31G(d) Density Functional Theory (DFT) calculations of **1** in an implicit solvent model for MeCN. (c) Calculated triplet potential energy surface. (d) Projected potential energy surface plot of key ground as well as triplet and quintet excited states involved in the proposed deactivation cascade which is indicated by green arrows; (c) and (d) adapted with permission from Fredin et al. [44] Copyright 2014 American Chemical Society.

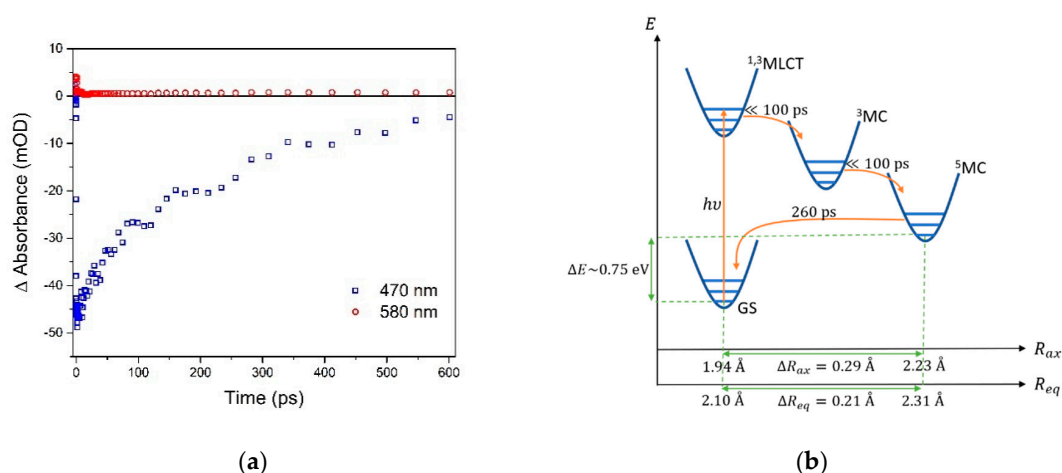


Figure 7. Photophysics of complex **2**. (a) Transient absorption kinetics of complex **2** following 480 nm excitation, recorded at 470 nm (blue squares) in the ground-state bleach region and at 580 nm (red circles) at the excited state absorption maximum. (b) Schematic representation of ground and excited state potential energy surfaces together with measured deactivation kinetics.

Complex **2**, featuring the same metal-carbene core as complex **1**, but with bulkier tert-butyl side-groups compared to methyl side-groups of complex **1**, in fact displayed more classic Fe photophysical behavior with ultrafast (sub-ps) deactivation to a meta-stable MC state with a ~ 260 ps ground state recovery (Figure 7). This result highlights the importance of steric effects of the bulky side-groups. In contrast, introduction of iso-propyl and hexanyl sidegroups (complexes **3** and **4**) did not influence the photophysics as much (Table 1) [31,56–58].

A combination of experimental time-resolved X-ray characterization and quantum chemical calculations was furthermore used to elucidate the nature of the $\tau \sim 260$ ps intermediate state of complex **2** [17]. This study provided more detailed insight into the photocycle of complexes with properties intermediate between Fe(II) complexes, featuring long-lived meta-stable high-spin ^5MC states on the one hand, and light-harvesting complexes such as complex **1** with excited CT excited

state lifetimes prolonged into the ps regime, on the other hand. The intermediate state, with a lifetime of 260 ps, was confirmed to be a ⁵MC state with significantly elongated M–L bonds and a significantly raised minimum energy compared to more conventional Fe-polyypyridyl spin crossover (SCO) complexes. A comprehensive understanding of the full photocycle of these complexes thus clearly benefits from emerging capabilities to complement traditional time-resolved optical measurements with time-resolved X-ray studies, providing information about structural changes around the metal core, local heating effects, etc. [27,39]

With a simple Fe(II)NHC core structure yielding significantly different photophysics compared to much studied Fe(II)polypyridyl complexes such as Fe(bpy)₃ and Fe(tpy)₂, complexes **1** and **2** have also received significant further attention in terms of advanced spectroscopic and computational investigations as prototype complexes for altered excited state dynamics. This is discussed further in Section 3.4 below.

3.2. Heteroleptic Fe^{II}-Bistridentate Complexes with Extended Absorption

In 2014, Duchanois et al. demonstrated that the absorption of Fe(II)NHC photosensitizers could be significantly extended to cover a broader range of the visible spectrum by combining complex **4** (a variation of the CNC-ligand in complex **1** with longer alkyl side-chains) in a heteroleptic complex **6** with a protonable pyridyl-terpyridine (pytpy) ligand (Figure 4) [58]. The protonated form **7** showed significant optical absorption features down to 590 nm, compared to 460 nm for the parent complex **4**. Accompanying quantum chemical calculations showed that the red-shifted optical absorption could be understood in terms of the lowest MLCT band featuring excitations to an energetically stabilized ligand-based π^* lowest unoccupied molecular orbital (LUMO), due to the extended π -conjugation on that ligand. Such demonstrated ability to tune absorption properties is an important stepping-stone for photosensitizer and photocatalytic applications, although still short lifetimes associated with a remaining tpy-type ligand (Table 1) remains an issue for any practical applications. Figure 8 illustrates how selected ligand motifs, including the low π^* with the protonated pytpy-ligand heteroleptic complex **7**, can be used to rationally influence the photo(electro)chemical properties of the FeNHC complexes. More recently, Zimmer et al. came to a similar conclusion with complexes **9** and the corresponding methylated complex **10** [56].

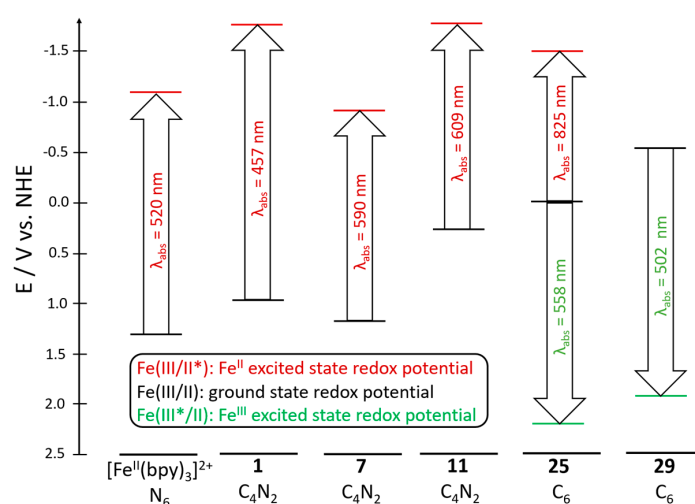


Figure 8. Photo(electro)chemical properties of selected FeNHC complexes (**1**, **7**, **11**, **25**, and **29**) discussed in the text, correlating estimated excited state redox potentials with the Fe(III/II) ground state redox levels as well as measured Fe(II) or Fe(III) excitation energies. Note that simple estimates of the excited state redox potentials are given from the lowest absorption features for the complexes. These values are used mainly for systematic comparative purposes, but neglect losses due to excited state relaxation (generally unknown for the non-emissive complexes).

3.3. Heteroleptic Fe^{II}-Trisbidentate Complexes

Investigations into an alternative type of heteroleptic complex **11** (Figure 4) were initiated in 2015 by Liu et al. based on trisbidentate binding with one traditional bpy ligand together with two bis-triazole mesoionic (MIC) ligands [61]. This yielded a ³MLCT excited state lifetime of 13 ps in solution (Table 1), which is an increase compared to the corresponding excited state lifetime of 9 ps that was reported for complex **1**. The most important significance of this complex was arguably the demonstration of competitive photophysical properties with an alternative arrangement of the four Fe-C bonds on two ligands. This leaves one bpy for further modification, either towards a wide range of bpy derivatives (e.g., with anchor groups, rods, or electron donating/withdrawing groups), or for further substitution with other ligand types such as further NHC ligands (see the discussion about the hexa-NHC complex **25** below). Additionally, complex **11** shows a quite broad range of CT absorption bands in the 300–700 nm range of the visible spectrum (Figure 5), as well as a negatively shifted Fe(III/II) reduction potential (listed in Table 1 and illustrated in Figure 8). The combination of a negatively shifted Fe(III/II) reduction potential together with the presence of a regular bpy ligand is consistent with the broad absorption extending to ca 700 nm in terms of MLCT excitations from high-energy t_{2g} levels on the metal to the regular bpy-π* ligand level. As illustrated in Figure 8, this shifting of the t_{2g}-levels thus provides another path to tune the photophysical properties in a favorable way [62].

3.4. Hot Branching and Wave Packet Dynamics

A couple of recent advanced time-resolved X-ray spectroscopy investigations have shed further light on the detailed deactivation mechanism of the prototype Fe(II)NHC complexes with excited state lifetimes in the ~10 ps range. The initial time-resolved optical investigations had focused on establishing the main timescale for deactivation, as well as to confirm the main charge-transfer nature of the excited state using complementary spectroscopic and computational methods. However, the proportions of the deactivation mechanism remained elusive, including the role of any parallel transient passage via MC scavenger states as part of the deactivation cascade. Tatsuno et al. recently provided direct spectroscopic evidence for the involvement of (intermediate-spin) ³MC states as an ultrafast (~150 fs) minority deactivation channel in hot branching dynamics following the initial photoexcitation of complex **11**, in addition to confirming the main channel (70%) population of the anticipated relaxed ³MLCT state with a 7.6 ps lifetime (Figure 9a,b) [67]. The detailed analysis also provided a timescale for the final ground state recovery step of ~2 ps. This reaffirms the main conclusions of the initial investigations pointing to the main part of the excited state population of the photochemically relevant ³MLCT state, while significantly enriching the understanding of other fast dynamics that with non-negligible contributions can impact the applications of these molecules.

A recent study of the ultrafast X-ray dynamics by Kunnus et al. additionally highlighted wave packet oscillations on a sub-ps timescale as part of the initial photophysical relaxation dynamics in complex **1**, i.e., in another of the early prototype FeNHC complexes with a ~10 ps ³MLCT lifetime (Figure 9c) [68]. They concluded that these oscillations are launched from the ultrafast population of a ³MC state from the initially populated MLCT state and with a characteristic frequency of 3.5 THz and a characteristic decay time of 500 fs. The oscillations were analyzed with a multitude of methods from optical transient absorption, over X-ray spectroscopy using the characteristic line shapes and intensity to the structural investigation with X-ray diffuse scattering. The perfect correlation between the methods that primarily probe the structure, the electronic structure and the spin momentum nicely illustrates the strong correlation and influence of the covalency.

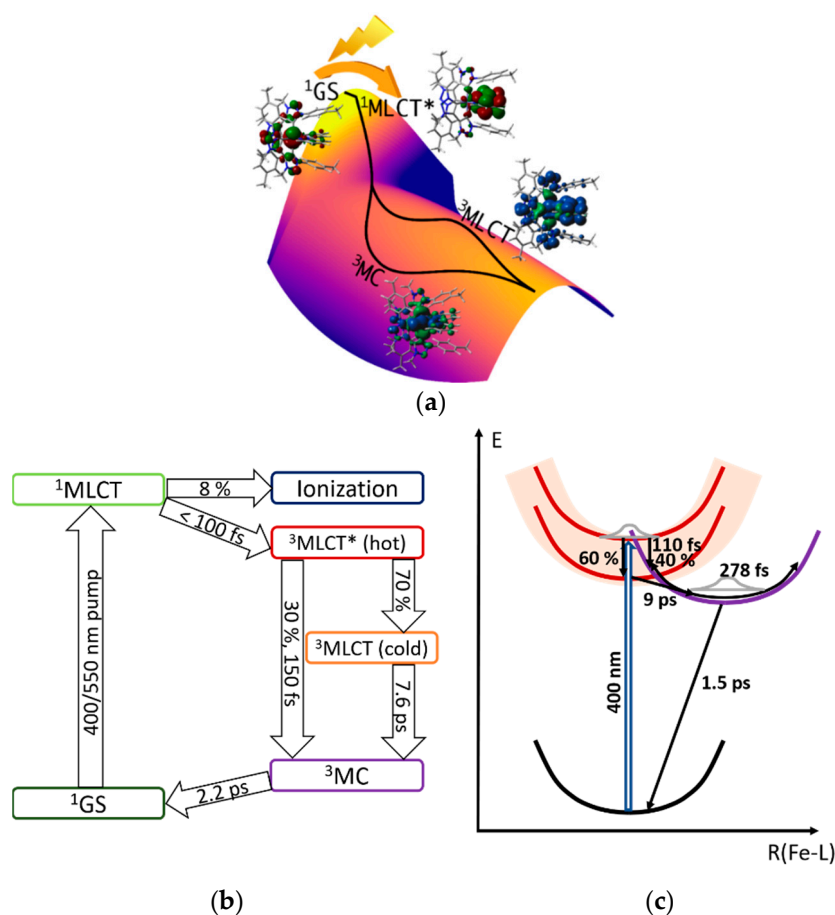


Figure 9. Schematic representations of advanced photoinduced dynamics probed using time-resolved X-ray spectroscopy. (a) Hot branching dynamics of complex **11** according to [67] displaying the evolution of the spectral shift of the measured TR-XES data over time together with associated electronic structure properties of the excitation process and branching states; (b) associated scheme summarizing the measured deactivation kinetics; (c) vibrational wave packet dynamics of complex **1** according to [68].

Further advanced computational investigations, including high level calculations of excited states as well as quantum dynamics simulations, have also been carried out recently by several groups to elucidate different aspects of the excited state properties of the iron carbene reference compounds and related iron complexes, with a range of different ligands from regular polypyridyls to NHCs and other strong σ -donors, see e.g., [21,24,69–74]. These studies provide fundamental insight into the difference of the FeNHC complexes compared to more traditional iron polypyridyl complexes such as $[\text{Fe}(\text{bpy})_3]^{2+}$, e.g., in terms of the role of intersystem crossing and transitions from CT to MC states. [45–47] These advanced calculations are often particularly valuable as a complement to sophisticated experimental investigations of ultrafast dynamics, including time-resolved X-ray dynamics probing of the metal-ligand and complex-solvent interactions [24,39,67,75].

3.5. Ligand Modifications

Further advancement of the photophysical properties of novel Fe(II)NHC complexes were reported in 2016, in particular reporting new record $^3\text{MLCT}$ excited state lifetimes up to 26 ps for free iron carbenes in solution (Table 1) [31,59,62]. This was achieved through modification of the CNC ligands by exchanging the imidazole moieties by more extended benzimidazole versions (complexes **12** and **13** in Figure 4), also including complexes **5** and **14** carrying carboxylic acid groups on the central pyridine rings together with imidazole and benzimidazole groups. Extending the π -system of the ligand (from

imidazole to benzimidazole) resulted in a stabilization of both t_{2g} (HOMO) and ligand-based LUMO levels. The net effect of these two shifts was a blue shift of the MLCT absorption (Table 1). However, adding carboxylic groups to a complex resulted in a red-shifted absorption compared to the parent complex which is indicative of a stabilization of the ligand-based LUMO level. Since the LUMO level is stabilized for both cases, it is plausible that the extension of the $^3\text{MLCT}$ excited state lifetime going from i.e., complex **1** \rightarrow **12** \rightarrow **14** is due to a stabilization of the CT state relative to the intermediate- and high-spin MC scavenger states. Calculations in reference [62] further suggested that the relaxed ^3MC state could even be higher than the $^3\text{MLCT}$ state energy, although the still quite short excited state lifetime in the 10's of ps is much shorter than many Ru(II) polypyridyl complexes, where such a favorable energetic ordering of the states seems more plausible. Calculations of relative energies of states of different characters are non-trivial, and further benchmarking and experimental verifications of such elusive states will be valuable to gain a more reliable understanding of the detailed excited state energy surfaces in future work.

Excited state lifetimes in solution were extended beyond 30 ps in the homoleptic Fe(II) complex **15** and 20 ps in the related complex **16** (structures shown in Figure 4, and photophysical properties listed in Table 1) [63]. The series of complexes **15**–**18** studied in this work all contained CNC-type ligands in which the central pyridyl group was replaced by a π -deficient diazanyl unit, and flanked by benzimidazole and imidazole carbenes, respectively. Following ultrafast relaxation, including ISC from an initially populated hot $^1\text{MLCT}$ state, the final long-lived component of ~ 32 ps in complex **15** was attributed to the transition from a ($^3\text{MLCT}/^3\text{MC}$)_{eq} mixed equilibrium state back to the ground state, based on the combined information from time-resolved spectroscopy and quantum chemical calculations of excited state energy pathways. In this model, the lifetime properties are explained by a small excited state barrier towards deactivation at extended Fe–N distances.

3.6. Coordination Arrangement- Isomerism and Carbene Count

A novel set of tris-bidentate pyridyl-NHC (PyNHC) complexes **19** and **20** (Figure 4) was investigated spectroscopically and computationally to find out the influence of the Fe–C arrangement in different *mer/fac* isomers. The *mer* form was identified from the synthesis of complex **19**, while synthesis of the hemicage complex **20** restricts the geometry to the *fac* form [64,65]. Significant complexity and isomer-specific differences were found in the deactivation dynamics for the two complexes. In particular, the complex spectral dynamics were explained using a model with parallel excited-state deactivation pathways (Figure 10a). According to this model, the complexes achieved different initial populations of two distinct triplet excited states ($^3\text{T}_1$ and $^3\text{T}_2$), characterized by different ground state recovery owing to differences in their triplet potential energy surface (PES) topologies (Figure 10b).

The specific arrangement of the Fe–C bonds appears to be an important factor that distinguishes the different *fac/mer* isomers of the complexes with the three carbenes around the Fe core. These complexes can either feature three N–Fe–C axes, or contain at least one N–Fe–N axis with potentially weaker σ donation. The latter case corresponds to an asymmetrical ligand field with potentially more facile distortions to MC scavenger states, similar to what has been discussed for other strong Fe–C σ -donation ligands [45].

Zimmer et al. were able to further elaborate on the influence of the NHC count on the photophysical properties of FeNHC complexes using a series of complexes (**3**, **21**, **22**, and **23**; chemical structures shown in Figure 4), covering cases with two, three, and four NHC groups [57,60]. Using a combination of ground state electronic structure characterization, time-resolved optical spectroscopy, and calculations' clear trends in the excited-state properties, including systematic shifts in frontier levels as well as excited-state lifetimes, could be elucidated. Also, Duchanois et al. made a similar observation (with complex **24**), concluding that at least four carbene bonds are needed to avoid the $^3\text{MLCT}$ -quenching spin cross over process as discussed in their review [31].

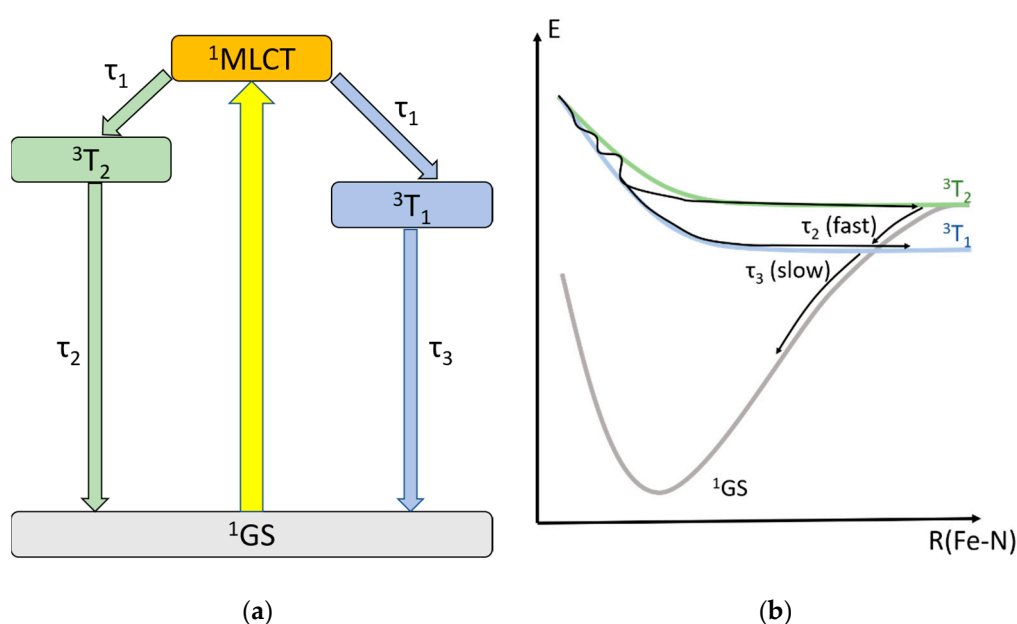


Figure 10. Excited state deactivation schemes for Fe(II)NHC *fac/mer* isomers of complexes **19** and **20**, highlighting the evidence for ground state recovery via two different triplet states (3T_1 and 3T_2) that are formed on ultrafast timescale (τ_1) and show ground state recovery with different timescales; τ_2 and τ_3 , respectively. (a) Deactivation scheme. (b) Jablonski diagram.

3.7. Hexa-Carbene Complexes

The hexa-carbene complex **25** (Figure 4) was developed as a further step towards iron-based light-harvesting complexes with stronger σ -donation compared to the previously discussed complexes with a mixture of Fe–C and Fe–N bonds with up to four carbene groups. The full carbene coordination resulted in a significantly more easily oxidized Fe-complex, spontaneously forming a Fe(III) complex under ambient conditions in acetonitrile solution (see discussion of Fe(III) complexes in Section 4 below), but also possible to isolate and investigate spectroscopically as the Fe(II) form of complex **25** [66]. The further destabilization of the t_{2g} levels of this Fe(II) complex (Figure 8) yielded a broad visible absorption extending towards the near-IR region (Figure 11a), resulting in an impressive 3MLCT excited state lifetime of ~ 0.5 ns (Table 1). The absorption extending far to the red also illustrates the gradual shifting of the absorption threshold to lower energies in different Fe(II)NHC complexes as the gap between the t_{2g} and π^* levels is reduced, as shown in Figure 5.

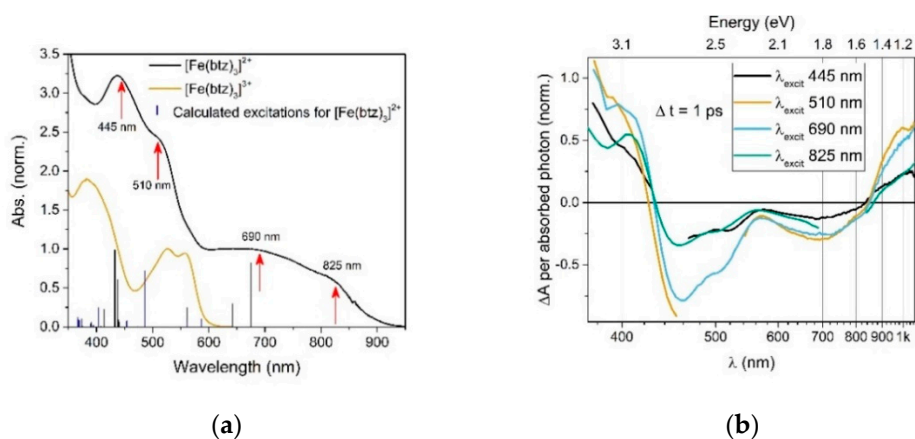


Figure 11. Cont.

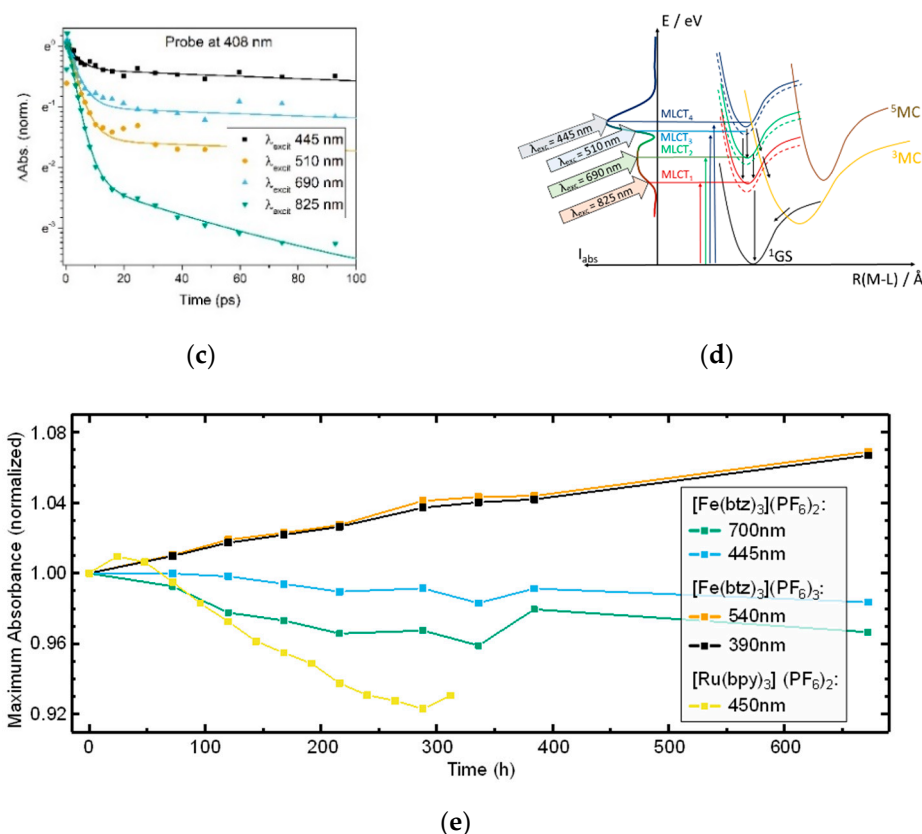


Figure 11. Band-selective photophysics of complex **25(II)**, investigated by Chábera et al. [76]. (a) Steady-state spectra of complex **25** in oxidation states **II** and **III** in acetonitrile. The red arrows indicate the excitation wavelengths for transient absorption experiments. (b) Transient absorption spectra of complex **25(II)** recorded 1 ps after excitation, normalized by the number of absorbed photons per cm^2 at each respective excitation wavelength (λ_{excit}). The x-axis (wavelength) is in reciprocal values (linear steps in energy). (c) Comparison of complex **25(II)** kinetics following excitations at different wavelengths (see legend) for kinetics recorded at 408 nm. Note that the graph shown in (c) is plotted in $\Delta A(\text{ln})/\text{Time}(\text{lin})$ scale. The kinetics have been normalized for visual clarity and the solid lines represent the fits. (d) Excited state manifold in the charge-transfer excitation energy region for complex **25(II)**, indicating the different excitation energies/wavelengths employed experimentally to probe the excited state dynamics (red, green, light blue and blue arrows), as well as selected potential decay paths (black arrows). Singlet and triplet forms of representative MLCT states in the charge-transfer manifold energy region are distinguished as solid and dashed lines, respectively. (e) Long-term photostability of **25(II)** and **25(III)**. Minor deviations from initial maximum absorption ($<10\%$ after 600 h continuous irradiation), associated with minor degradation and/or solvent evaporation. Results in **a–d** adapted with permission from ref [76], published by The Royal Society of Chemistry.

Furthermore, the broad visible absorption comprising several CT bands facilitated a more thorough recent investigation of the excited state dynamics of complex **25(II)**, using time-resolved optical spectroscopy (Figure 11). These investigations showed that while most of the observed dynamics on the 100's of ps timescale follow the same trends as initially presented by Chábera et al. [66], a closer inspection of the time-resolved dynamics reveal interesting band-selective variations in the dynamics on the sub-100 ps timescale that deserve further investigation [76].

3.8. Molecular Photovoltaics

An early envisioned application of the iron-carbene photosensitizers was for usage in dye-sensitized solar cells (DSSC) [9]. In a DSSC, the photosensitizer is attached to a semiconductor, to which charge carriers (typically electrons for n-type semiconductor sensitization) can be transferred

from the excited molecule. [35,77,78] The charge carriers are extracted via an electrode, and a full cell is constructed with additionally one counter-electrode and a redox mediator. A photovoltage is created under illumination, allowing a current to be extracted from the DSSC, see Figure 12 [79].

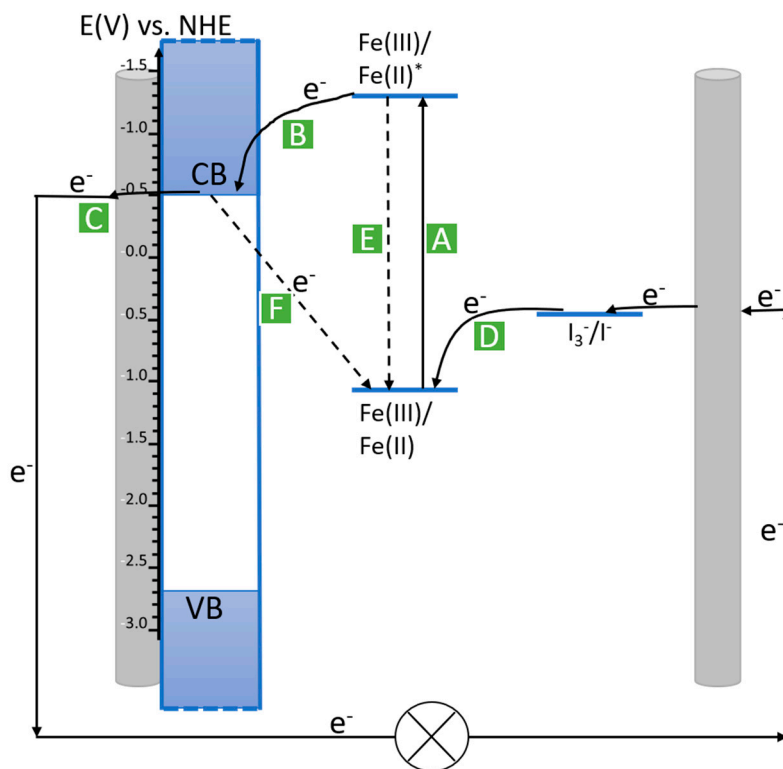


Figure 12. Schematic of an n-type dye-sensitized solar cell (DSSC) with incorporated redox potential scale. Fe(III)/Fe(II) is here exemplified by specific reduction potential for complex 5 as the photosensitizer, with Fe(III)/Fe(II)^* as the corresponding excited state potential. I_3^-/I^- is used as the redox mediator and TiO_2 as the semiconductor (CB—conduction band, VB—valence band). Key processes in the DSSC marked in the figure are: A—excitation, B—injection, C—extraction, D—regeneration, E—relaxation, F—recombination.

Several requirements need to be met for a photosensitizer to work in a DSSC arrangement. Firstly, the photosensitizer must bind to the semiconductor, which is typically accomplished using dedicated anchor groups [80]. Secondly, the photosensitizer needs to absorb visible light and preferably with a high extinction, even though the nanostructured TiO_2 electrodes are designed to allow for efficient light-harvesting, due to the large surface sensitization area. Photosensitizers must also be able to inject charge carriers efficiently, including sufficient excited state lifetime and appropriate positions of ground and excited state redox levels to drive interfacial injection and regeneration from the redox couple. Finally, the photoredox-stability of all states involved in the photocycle is important for the long-term performance of the device. It can be noted that some iron complexes predating the iron carbenes were investigated as photosensitizers for DSSCs [81–84]. These investigations provided insight into fast interfacial injection processes, but the sensitizers were never competitive for device applications, which in large part can be ascribed to the short excited state lifetimes and/or lack of photostability [22].

The first iron-carbene featuring anchor groups for attachment to a semiconductor surface, complex 5, reported in 2015 was a development of complex 1, where carboxylic groups have been attached to both pyridine rings (Figure 4) [59,85]. The addition of this electron-withdrawing group not only made the molecule suitable for surface sensitization [9], but also strongly redshifted the MLCT absorption maximum compared to complex 1, such that a big part of the visible region (350–550 nm, see Figure 5) is covered by complex 5 with a maximum extinction coefficient of $16200 \text{ M}^{-1} \text{ cm}^{-1}$ (Table 1) [59,85].

The alignment of the redox levels of complex **5** to the conduction band of the commonly used semiconductor TiO_2 shows that complex **5** could potentially inject electrons into the conduction band (see Figure 12) [59]. Such injection was shown to be very efficient (Figure 13a), and the fundamental injection mechanism was investigated using a combination of electron paramagnetic resonance, transient absorption spectroscopy, and ultrafast time-resolved terahertz spectroscopy [85]. The observed kinetics are summarized in Figure 13a, with the key message that an MLCT lifetime on the order of tens of ps is enough to inject electrons with high efficiency. This could be seen as constituting a significant stepping-stone towards the broader usefulness of iron-based photosensitizers [12,13].

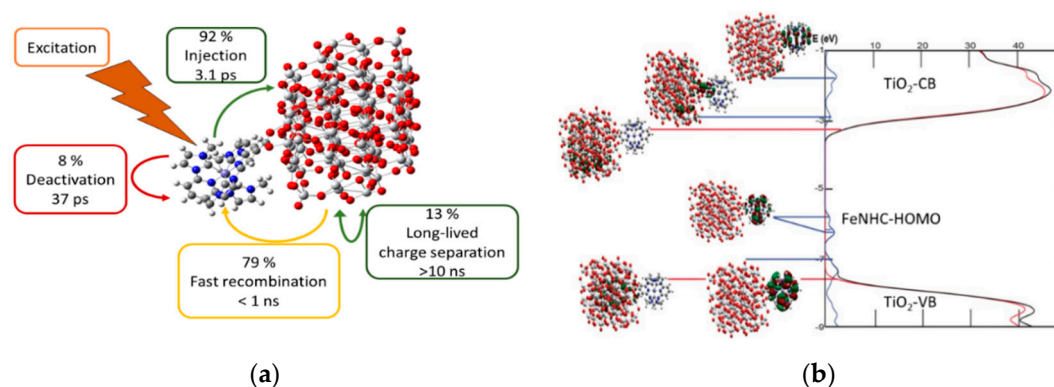


Figure 13. (a) Measured interfacial injection dynamics of complex **5** sensitized to a surface of nano- TiO_2 according to results from Harlang et al. [85], and (b) associated calculated interfacial electronic structure properties. Adapted with permission from Fredin et al. [86], published 2016 with copyright by Wiley.

The fundamental suitability of the interfacial electronic properties, in terms of dye-semiconductor level alignments and interfacial electronic coupling, was also corroborated by explicit atomistic quantum chemical calculations (Figure 13b) [86]. Further combined computational studies with DSSC performance characterization, including considerations of protonation/deprotonation effects and possibilities for further heteroleptic design strategies, were presented by Pastore et al. [32] Jakubikova and co-workers further investigated FeNHC- TiO_2 interfaces as part of a series of Fe-based sensitizers for DSSC applications using quantum dynamics simulations, e.g., highlighting the importance of conformational sampling on the interfacial electron transfer characteristics [87–89].

A first attempt of using complex **5** as a sensitizer in DSSCs was made in the work from 2015 by Duchanois et al. [59] The I_3^-/I^- couple was used as a redox mediator, and complex **5** was co-adsorbed onto TiO_2 together with chenodeoxycholic acid. Despite a low overall conversion efficiency (0.13%), the incident photon-to-current conversion efficiency (IPCE) showed a significant contribution to the current generated from the spectral region where complex **5** absorbs. A proof of principle was thus shown for the FeNHC DSSC, with the main parameter limiting the DSSC performance identified as the low short-circuit current density [59]. This shortcoming in device performance corresponds well on a molecular level with the deleterious recombination processes observed in the time-resolved interfacial electron transfer experiments discussed above [85].

In 2016, DSSCs were presented that had been fabricated with complexes **14**, **26**, **27**, and **28** as photosensitizers (Figure 4). Complex **14**, despite a longer $^3\text{MLCT}$ lifetime compared to complex **5**, showed worse conversion efficiency than complex **5**, which was attributed to a worse attachment to the TiO_2 surface. From DFT calculations, the homoleptic complexes **5** and **14** seemed to not experience the desired electron flow from photosensitizer to TiO_2 . However, the calculations showed beneficial electron flows when deprotonating the carboxylic group not attached to TiO_2 , and ideas of heteroleptic design strategies were presented by Pastore et al. [32] The heteroleptic complexes **26–28**, with electron-donating groups incorporated to direct the electron flow, were synthesized and tested as photosensitizers in DSSC. Despite improved interfacial charge separation compared to the homoleptic

compounds, the heteroleptic complexes did not yield better conversion efficiencies (Table 2). The main limitation to the performance was attributed to recombination [32].

The current density of DSSCs with complex **5** as the photosensitizer was improved significantly in 2018 and further in 2019, by altering both solvent and additives (changing acetonitrile to 3-methoxypropanenitrile and adding an ionic liquid together with more Li⁺), but keeping the redox mediator (I₃⁻/I⁻). A new record conversion efficiency of 0.66% was obtained [90,91]. The current record conversion efficiency for FeNHC-based DSSCs, approaching 1%, was obtained yet more recently by Marchini et al. A blocking underlayer in the TiO₂ structure together with additives guanidinium thiocyanate and MgI₂ helped to stop recombination and accelerate the regeneration of the dye (redox mediator still I₃⁻/I⁻) [92]. Several important conclusions were drawn from transient absorption spectroscopy studies of transparent DSSC, with complex **5** as the photosensitizer. The charge separated state (e-(TiO₂)/Fe(III)) has a lifetime on the ms-timescale (in an inert electrolyte) both for Fe-based and Ru-based photosensitizers. With recombination taking place on a μs-timescale, improving this lifetime will not readily help. The recent study of recombination and regeneration dynamics of DSSCs with optimized I-V performance also showed the need to shield the photoanode, and highlighted several factors, including incomplete injection due to the competing relaxation process of the excited state as important aspects for further photosensitizer development [92].

Table 2. Best current solar cell characteristics for iron-carbenes reported as photosensitizers in DSSCs. Note that only DSSCs with complex **5** as photosensitizer have been subjected to significant optimization efforts beyond an initial DSSC performance characterization.

Photosensitizer	J _{sc} /mAcm ⁻²	V _{oc} /mV	Fill Factor	Conversion Efficiency/%	Ref
5	3.3	440	0.63	0.92	[92]
14	0.12	368	0.71	0.03	[32]
26	0.33	400	0.73	0.10	[32]
27	0.36	440	0.73	0.11	[32]
28	0.36	390	0.71	0.10	[32]

All in all, these initial studies of FeNHC complexes for photosensitization applications provide proof-of-principle demonstrations that FeNHC photosensitizers possess fundamentally viable photophysical properties to make functioning solar energy conversion devices relying on ultrafast charge separation. While a lot of further work is needed to optimize the still low power conversion efficiencies, the recent studies also show that these can indeed be improved through systematic optimization efforts.

4. Fe(III) Complexes

Several Fe(III) complexes with different types of ligands are known, though often with a high-spin (hextet) ground state corresponding to a half-filled d-shell and with less than ideal light-harvesting properties [93]. Some Fe(III) complexes with stronger σ-donating ligands have also previously been found to form low-spin (doublet) ground states, including a Fe(III) hexa-carbene species that had been previously synthesized in a different context that did not include investigation of photophysical properties [94].

Photoluminescent Fe(III) Hexa-Carbene Complexes

The novel Fe^{III}(btz)₃ hexa-carbene complex **25** (Figure 4), synthesized as a further development of the Fe^{II}(bpy)(btz)₂ complex **11**, readily formed in the Fe(III) oxidation state, [Fe^{III}(btz)₃]³⁺, as a stable species under ambient conditions [52]. This Fe(III) complex showed a remarkable case of weak but persistent photoluminescence from an excited state lifetime of 100 ps (Table 3) [52]. The ground state of the complex was assigned as a low-spin (doublet) d⁵ complex, with excitation

and photoluminescence involving transitions to and from an excited state characterized as a low-spin (also doublet) ligand-to-metal charge transfer ($^2\text{LMCT}$) state. The observation of photoluminescence is apparently facilitated by the spin-allowed fluorescence decay from the $^2\text{LMCT}$ state, which is different to the ultrafast ISC commonly encountered as singlet to triplet MLCT conversion in d^6 complexes. The doublet spin properties are seen to have a fundamental impact on the photophysics also in other ways, including a comparatively small observed Stokes' shift.

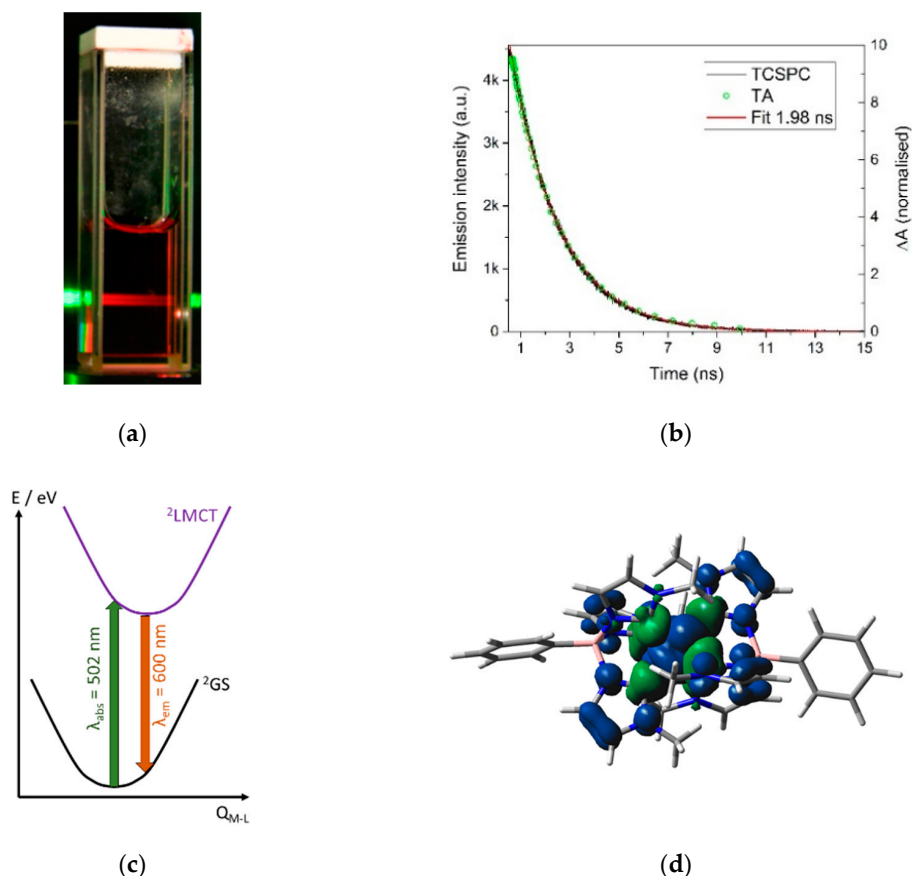


Figure 14. Photophysics and electronic structure properties of complex **29** [54]. (a) Photoluminescence of complex **29** under 502 nm irradiation; (b) ~ 2 ns lifetime measurements of complex **29** by transient absorption (TA) and time-correlated single photon counting (TCSPC). (c) Doublet ground state (^2GS) and ligand-to-metal charge transfer ($^2\text{LMCT}$) excited state potential energy landscape, including arrows indicating the doublet-doublet excitation and deactivation. (d) Ground state spin density from density functional theory calculations.

Table 3. Photo(electro)chemical properties of Fe(III)NHC complexes. All measurements in CH_3CN unless otherwise noted. Electrochemical measurements conducted in CH_3CN against $\text{Fc}^{+/0}$ and converted to corresponding standard NHE values using a standard reference electrode conversion constant of +0.630 V [55].

Complex	$\lambda_{\text{abs,max}}^{\text{a}}$ /nm	ϵ / $\text{M}^{-1}\text{cm}^{-1}$	τ_{LMCT} /ps	$\lambda_{\text{em,LMCT}}^{\text{b}}$ /nm	QY_{PL} /%	$E_{1/2}$ Fe(III/II) /V vs. NHC	$E_{1/2}$ Fe(IV/III) /V vs. NHC	Ref
25	384 (528, 558)	2400	100	600	0.03	0.05	^c	[53]
29	502	3000	1960	655	2.1	−0.53	0.88	[54]

^a The most intense LMCT peak. In case of significant LMCT peaks of lower energy, these are stated in parenthesis.

^b Highest energy emission peak. ^c Outside electrochemical window.

Further recent progress extended the $^2\text{LMCT}$ excited state lifetime of a Fe(III) d^5 complex into the ns timescales, and improved visible photoluminescence yield to $\sim 2\%$ in the bistridentate complex **29** (Figure 4) [53]. Photophysical properties of this complex are shown in Figure 14. Especially noteworthy was the demonstration that complex **29** is capable of driving bimolecular photoredox reactions, as discussed further below in Section 5. These excited-state properties were both unprecedented and unexpected for any iron complex, as the main focus had previously been to make Fe(II) analogues of the favorable photophysics of Ru(II) d^6 complexes. The $^2\text{LMCT}$ excited state is familiar from the excited states in the $\text{Fe}^{\text{III}}(\text{CN})_6$ complex, with prototype strongly σ -donating ligands [25], but going beyond monodentate ligands apparently does not only favor the formation of long-lived excited states but also result in complexes showing significant photostability against photo-induced ligand loss processes. This makes these complexes much more appealing as light-harvesters for photophysical and photochemical applications. A more detailed exploration of $^2\text{LMCT}$ excitations in d^5 complexes in general was recently reviewed separately [33].

The combination of the strongly σ -donating carbene ligands, together with the unconventional d^5 electronic configuration on the metal yielding improved excited state properties, also makes it interesting to investigate the ground and excited state electronic properties of these types of Fe(III) hexa-carbene complexes further. A first step in this direction was taken using a combination of X-ray spectroscopic characterization and quantum chemical calculations of complex **25(III)**, indicating strong metal-ligand bonding interactions [95]. These non-trivial metal-ligand bonding properties were further detailed in a recent study combining optical characterization with resonant photoemission X-ray spectroscopy of thin films of complex **25(III)**. [96] This study firstly confirmed the integrity of the Fe(III) oxidation state for thin films, thus broadening the potential range of viable applications towards thin film technologies significantly. Secondly, the presented X-ray spectroscopic results elucidated the involvement of the different ligand constituents to different molecular orbital components of the valence electronic structure in significant detail. In particular, this provided direct spectroscopic evidence for strong valence molecular orbital interactions between the Fe(III) center and the carbene ligands, in contrast to more independent side-group features.

5. Photocatalysis

Homogeneous (molecular) and heterogeneous catalysts based on iron and other Earth-abundant materials are of broad current interest for sustainable and environmentally friendly large-scale application [4,97–99]. Photoredox chemistry and photocatalysis in particular provide important avenues for water splitting in artificial photosynthesis, and related strategies to produce solar fuels such as methanol [1,100–103]. This includes a significant amount of interest and progress in exploring photocatalytic conversions involving iron complexes as recently reviewed [104]. As the short excited state lifetime of traditional iron complexes do not lend themselves well for use as light-harvesting complexes driving photoredox-processes, the focus has often been on photochemical reactions initiated by ligand-loss or ligand-fragmentation processes that can be triggered on ultrafast timescales [29,105].

Already, the moderate extended lifetimes of the early iron(II) carbene complexes prompted Zimmer et al. to investigate the potential of using homoleptic and heteroleptic Fe(II)NHC complexes **3** and **8** (Figure 4) as photosensitizers for light-induced water reduction [57]. For complexes **3** and **8**, turn-over numbers of 4 and 3 were obtained after 20 h of AM1.5 illumination. It was argued that the big difference in prize of different metals could largely offset the drawback of a moderate photocatalytic activity of 1:17, compared to a standard Ir-based photocatalytic complex, while pointing to the significant potential for iron-based photosensitizers with further extended excited state lifetimes. Also, the iron-based photosensitizers had better stability under photocatalytic conditions compared to the Ir polypyridyl complex they used as a reference. Pöpcke et al. also recently discussed some challenges and opportunities for using FeNHC complexes for homogeneous photocatalysis from the perspective of time-resolved investigations of the initial steps of such photo-induced processes [106].

Significant further improvement towards iron carbene based photocatalytic applications was recently reported using a Fe(III) bistridentate complex **29** (Figure 4) [53]. The improvement in photophysical properties in this complex builds on the successful application of negatively charged borate-containing ligands to further strengthen the ligand field strength in a favorable coordination environment [107]. As introduced above in Section 4, this complex was first shown to have remarkable photophysical properties for any iron complex in terms of a record excited-state lifetime of 2 ns and a photoluminescence quantum yield of ca 2% (Table 3 and Figure 14). It can be noted that the same ligand had previously been employed for photophysical purposes in a Mn(IV) bistridentate complex that displayed near-IR photoluminescence in the solid state at liquid nitrogen temperatures [108].

The ns excited state lifetime of complex **29**, together with significant photo-oxidation and photo-reduction potentials, were used to also demonstrate the capability to drive both photo-oxidation and photo-reduction reactions efficiently using prototype sacrificial electron donors (diphenylamine) and acceptors (methylviologen) in solution (Figure 15). For the case of complex **29** (Fe(III), Figure 15 right part), the excited state of the molecule leaves a vacancy in the ligand-based π -levels that can be reduced by an electron donor. Instead of being reduced, the excited molecule can be oxidized by donation of an electron from the t_{2g} -levels to an electron acceptor. The ground and excited state redox potentials of complex **29** are visualized in Figure 8 together with corresponding values for other selected FeNHC complexes. This highlights the significant excited state oxidation and reduction potential of complex **29** [54,109]. In particular, this includes a very strong photo-oxidizing capacity for the 2 LMCT state that emerges as a common feature, together with a few earlier known photoredox-active Tc(II) and Re(II) complexes [110–112].

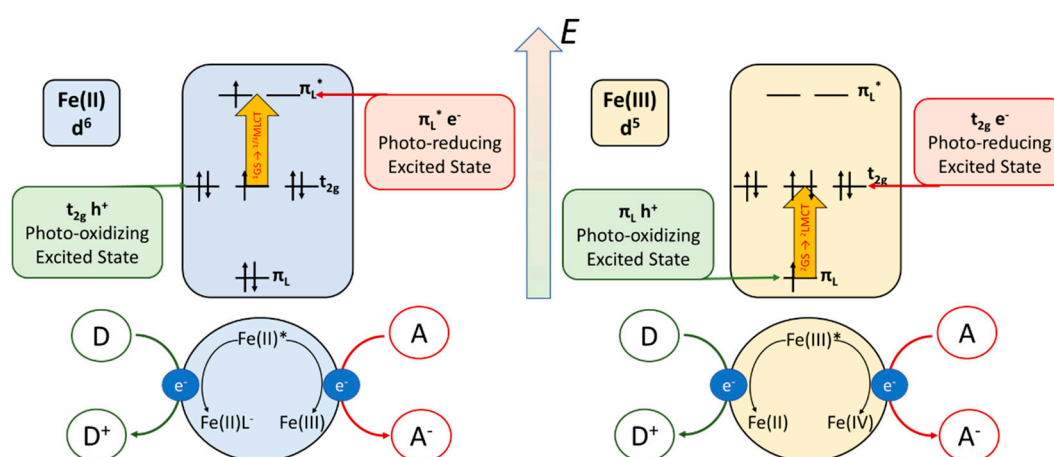


Figure 15. Fundamental photoredox processes for Fe(II)/ d^6 (left) and Fe(III)/ d^5 (right) systems. Note that the different excitation processes involve different ligand orbitals that contribute to making the Fe(II)/MLCT and Fe(III)/LMCT cases fundamentally different in terms of excited state oxidation and reduction capabilities.

A generalized kinetics schematic for bimolecular photoredox-quenching involving an Fe(III) light-harvesting complex and an electron donor as quencher (Q) is shown in Figure 16. This includes the typical photo-excitation and bimolecular diffusion limited (or alternatively static) quenching, together with charge separation (CS) and a subsequent competition between charge recombination (CR) or photoproduct formation. Due to the open-shell (doublet) ground and excited state electronic structure properties of the Fe(III)/ 2 LMCT complexes, the full photocycle must be considered in the light of the special properties of the doublet spin states involved. Further investigations of both the early photoinduced reaction steps using time-resolved spectroscopic techniques, as well as identification and optimization of a variety of photoproducts associated with different photocatalytic targets towards artificial photosynthesis, solar fuels and organic photochemistry/photocatalysis, constitute obvious

lines for further research, based on the recent proof-of-principle demonstration of driving photoredox processes by Kjær et al. [53]

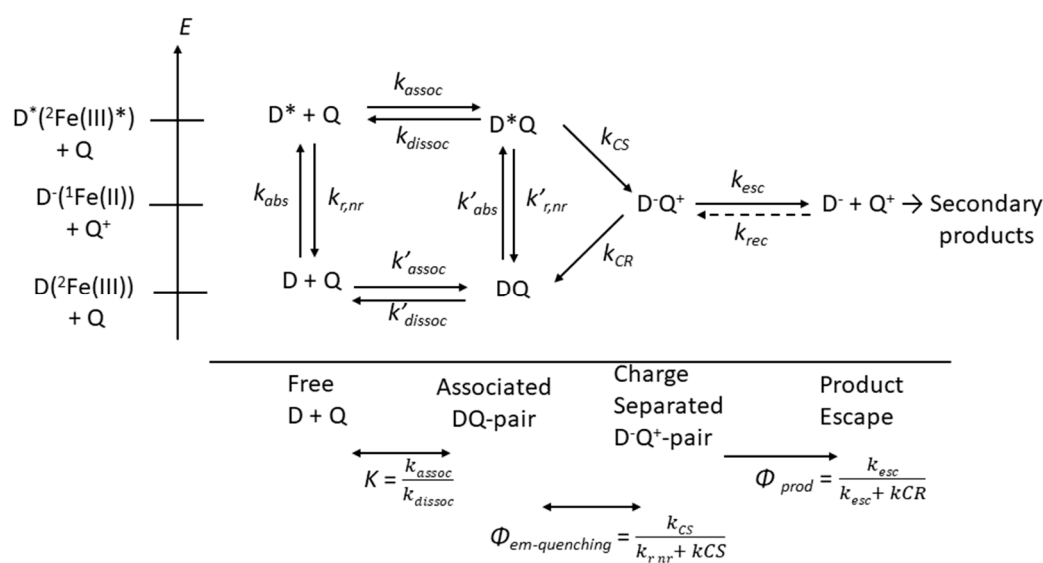


Figure 16. Photoinduced bimolecular kinetics involving the unconventional photoexcited ²LMCT state of a Fe(III)NHC complex. From left to right, the scheme illustrates photo-excitation of the light-harvesting complex, formation of a donor-acceptor pair involving the excited complex, followed by charge separation (CS) as well as charge recombination (CR), in competition with the ultimate long-lived photoproduct formation associated with solvent cage escape. This illustrates a case of oxidation and subsequent re-reduction or photoproduct formation of a sacrificial electron donor that gives a full photocycle, in which all steps are overall doublet states without any intersystem crossing or spin forbidden transitions.

Another strategy towards photocatalytic applications involving noble-metal-free dyads for heterobimetallic devices was recently presented by Zimmer et al. using a heteroleptic Fe(II) complex connected via a polypyridyl linker to a Co dimethylglyoxime motif in complex **30** (Figure 4) [54]. This first work in this direction focused on characterizing photophysical properties associated with the heterobimetallic system in itself, as well as solvent influences on the photophysical properties. Further work in this direction provides a promising path towards the design of improved photofunctionality, in which light-harvesting capabilities of FeNHCs can be combined with known catalytic functions of other metal centers.

Bichromophoric Fe(II)NHC complexes coupled to an anthracene organic electron acceptor were also recently studied theoretically by Francés-Monerris et al., providing insight into the role of the bridging unit to influence the photophysical properties of such bichromophoric assemblies of potential interest for photocatalytic applications [113].

Overall, the noticeable progress in the fundamental photophysical properties of the FeNHC complexes compared to more traditional Fe polypyridyl and related complexes in terms of ns excited state lifetimes and high photo-oxidation and photo-reduction potentials opens up a new field for iron-based molecular photocatalysis. At the same time, it is clear that this research direction is still very much in its infancy, with only a few proof-of-principle demonstrations of fundamental applicability towards photocatalysis. Many further investigations can therefore be anticipated to be of interest for the near future. This includes further design and development of new complexes with modified photocatalytic properties such as tuning of excited state oxidation and reduction potentials, as well as a broader range of investigations to expand on the applicability in different kinds of photocatalytic reactions e.g., towards solar fuels or towards organic conversion reactions.

Finally, the new and largely unexplored photochemical properties of the Fe(III)NHC complexes provide an interesting area for fundamental studies of photocatalytic reaction mechanisms featuring the unconventional $^2\text{LMCT}$ excited state. Given the promising excited state properties of this type of low-spin LMCT photochemically active complexes, combined with overall scarcity of other examples of such photoredox-processes in general (mainly limited to a few examples involving rare Tc(II) and Re(II) complexes [110,111,114]), this provides an important area for further investigations that has the potential to be of broader interest beyond the Fe(III)NHC complexes.

6. Outlook and Conclusions

Significant progress towards making iron complexes useful for light-harvesting in solar energy conversion as well as photocatalysis has been made in the last decade, triggered by significant extensions of excited state lifetimes of high energy charge transfer states in iron carbenes complexes. Noteworthy milestones (Figure 2) that have been highlighted in this review include reaching excited state lifetimes of charge transfer states in the nanosecond regime, achieving photoluminescence under ambient conditions in solution, and the demonstration of efficient semiconductor sensitization in terms of efficient interfacial electron transfer for molecular photovoltaic applications, as well as proof-of-principle demonstrations of working DSSC devices. In the context of carbene-based catalysts, recent demonstrations of significant photo-oxidation and photo-reduction offers an important stepping-stone towards utilization of Earth-abundant FeNHC complexes for photocatalytic applications. This includes key opportunities towards challenging artificial photosynthesis and solar fuel applications, judging by the wide range of excited state oxidation and reduction potentials that can be reached for light-harvesting complexes with substantial excited state lifetimes. Interestingly, a very recent report of another class of iron(II) complex with unconventional ligand structure showed favorable light-harvesting, and excited state lifetime reaching the nanosecond milestone further opening up the field for iron-based light-harvesters and photocatalysts [115]. Some progress has also been made to develop and characterize cyclometallated Fe complexes as a conceptually related strategy to introduce strongly σ -donating Fe–C bonds, that with further improvements may widen the field of potential Fe-based light-harvesting complexes for solar energy conversion and photocatalytic applications [116].

One of the most surprising recent developments that has contributed significantly to broadening the potential scope of the photophysics and photochemistry for iron-based photoconversion applications has been the discovery and utilization of $^2\text{LMCT}$ states in Fe(III) (d^5) complexes. This kind of excitation has fundamentally different and still quite unexplored electronic and spin properties, but the reverse charge transfer direction creates opportunities for highly photo-oxidizing processes as well as alternative charge-transfer applications, such as interfacial hole extraction, instead of electron injection that may be relevant both for molecular photovoltaics and hybrid photocatalytic applications. Further work to explore how far the different types of iron-based photocatalysts can be developed will now be interesting, both in terms of fundamental photophysical properties as well as innovative photochemical applications.

All together, the recent progress with photofunctional iron carbene complexes discussed in this review, including both Fe(II) and Fe(III) species, has opened-up a range of interesting new possibilities for further development of solar energy conversion and photocatalysis. First, this includes significant openings to develop applications based on the FeNHC complexes themselves. There are also increasing signs that the early progress towards photofunctional iron complexes where the iron carbenes paved the way over the last several years is now ripe to be broadened, through introduction of other types of advanced ligand design motifs promoting favorable photophysical and photochemical properties. This sets the stage for interesting comparisons of different classes of photoactive iron complexes that are becoming available. Finally, the iron carbene complexes discussed in this review contribute to a broader current trend to develop challenging photosensitization and photocatalytic applications, based on a broader selection of first row Earth-abundant metals for large-scale applications. Here, the recent progress with FeNHC and other strongly σ -donating ligands elevates it to a select group of

transition metals, including also Ti, Cr, Co, Cu and Zn, that are simultaneously relatively abundant and with interesting photocatalytic and solar energy conversion potential [2–4,6,117]. Given overlapping technological interests, and to some extent common scientific challenges, for these elements it seems likely that there can be extensive opportunities to combine progress and develop common strategies for complexes based on these abundant first row transition metals.

All this adds up to placing the iron carbenes in the middle of a vibrant field of current research to develop Earth-abundant transition metal complexes for solar energy conversion and photocatalytic applications more broadly. It therefore looks exciting to pursue further progress for iron carbenes and related complexes, both in terms of continued improvements of the fundamental photophysical and photochemical properties, as well as to continue recently initiated developments towards innovative solar energy conversion and photocatalysis technologies.

Author Contributions: All authors contributed actively to the writing of this review. All authors have read and agreed to the published version of the manuscript.

Funding: This research was funded by the Swedish Energy Agency (STEM), the Swedish Strategic Research Foundation (SSF), the Knut and Alice Wallenberg (KAW) Foundation, and the Swedish Research Council (VR) for support. The Swedish National Supercomputing Centers LUNARC and NSC are gratefully acknowledged for providing computing resources via NSC. N.W.R. gratefully acknowledges funding from the Alexander von Humboldt Foundation within the Feodor–Lynen Fellowship program.

Acknowledgments: We gratefully acknowledge many valuable discussions and constructive collaborations with all co-workers in Lund and internationally.

Conflicts of Interest: The authors declare no conflict of interest.

References

1. Gray, H.B.; Maverick, A.W. Solar Chemistry of Metal Complexes. *Science* **1981**, *214*, 1201–1205. [[CrossRef](#)]
2. Bozic-Weber, B.; Constable, E.C.; Housecroft, C.E. Light harvesting with Earth abundant d-block metals: Development of sensitizers in dye-sensitized solar cells (DSCs). *Coord. Chem. Rev.* **2013**, *257*, 3089–3106. [[CrossRef](#)]
3. Wenger, O.S. Photoactive Complexes with Earth-Abundant Metals. *J. Am. Chem. Soc.* **2018**, *140*, 13522–13533. [[CrossRef](#)]
4. Dalle, K.E.; Warnan, J.; Leung, J.J.; Reuillard, B.; Karmel, I.S.; Reisner, E. Electro- and Solar-Driven Fuel Synthesis with First Row Transition Metal Complexes. *Chem. Rev.* **2019**, *119*, 2752–2875. [[CrossRef](#)]
5. Glaser, F.; Wenger, O.S. Recent progress in the development of transition-metal based photoredox catalysts. *Coord. Chem. Rev.* **2020**, *405*. [[CrossRef](#)]
6. Förster, C.; Heinze, K. Photophysics and photochemistry with Earth-abundant metals – fundamentals and concepts. *Chem. Soc. Rev.* **2020**, *49*, 1057–1070. [[CrossRef](#)]
7. Balzani, V.; Bergamini, G.; Campagna, S.; Puntoriero, F. Photochemistry and photophysics of coordination compounds: Overview and general concepts. *Top. Curr. Chem.* **2007**, *280*, 1–36. [[CrossRef](#)]
8. Campagna, S.; Puntoriero, F.; Nastasi, F.; Bergamini, G.; Balzani, V. Photochemistry and photophysics of coordination compounds: Ruthenium. *Top. Curr. Chem.* **2007**, *280*, 117–214. [[CrossRef](#)]
9. Liu, Y.; Persson, P.; Sundström, V.; Wärnmark, K. Fe N-Heterocyclic Carbene Complexes as Promising Photosensitizers. *Acc. Chem. Res.* **2016**, *49*, 1477–1485. [[CrossRef](#)]
10. Abrahamsson, M. Solar energy conversion using iron polypyridyl type photosensitizers—A viable route for the future? In *Photochemistry*; Albini, A., Fasani, E., Eds.; RSC: London, UK, 2017; pp. 285–295. [[CrossRef](#)]
11. Wenger, O.S. Is Iron the New Ruthenium? *Chem. A Eur. J.* **2019**, *25*, 6043–6052. [[CrossRef](#)]
12. Motley, T.C.; Meyer, G.J. Are we on a path to solar cells that utilize iron? *NPG Asia Mater.* **2016**, *8*, e261. [[CrossRef](#)]
13. Galoppini, E. Light harvesting: Strike while the iron is cold. *Nat. Chem.* **2015**, *7*, 861–862. [[CrossRef](#)]
14. Boillot, M.L.; Weber, B. Mononuclear ferrous and ferric complexes. *Comptes Rendus Chim.* **2018**, *21*, 1196–1208. [[CrossRef](#)]
15. McCusker, J.K. Electronic structure in the transition metal block and its implications for light harvesting. *Science* **2019**, *363*, 484–488. [[CrossRef](#)]

16. Mccusker, J.K.; Vlcek, J. Antonin, Ultrafast Excited-State Processes in Inorganic Systems. *Acc. Chem. Res.* **2015**, *48*, 1207–1208. [[CrossRef](#)]
17. Zhang, E.; Gaffney, K.J. Mechanistic studies of photoinduced spin crossover and electron transfer in inorganic complexes. *Acc. Chem. Res.* **2015**, *48*, 1140–1148. [[CrossRef](#)]
18. Auböck, G.; Chergui, M. Sub-50-fs photoinduced spin crossover in $[\text{Fe}(\text{bpy})_3]^{2+}$. *Nat. Chem.* **2015**, *7*, 629–633. [[CrossRef](#)]
19. Zhang, W.; Alonso-Mori, R.; Bergmann, U.; Bressler, C.; Chollet, M.; Galler, A.; Gawelda, W.; Hadt, R.G.; Hartsock, R.W.; Kroll, T.; et al. Tracking excited-state charge and spin dynamics in iron coordination complexes. *Nature* **2014**, *509*, 345–348. [[CrossRef](#)]
20. Zhang, W.; Kjær, K.S.; Alonso-Mori, R.; Bergmann, U.; Chollet, M.; Fredin, L.A.; Hadt, R.G.; Hartsock, R.W.; Harlang, T.; Kroll, T.; et al. Manipulating charge transfer excited state relaxation and spin crossover in iron coordination complexes with ligand substitution. *Chem. Sci.* **2017**, *8*, 515–523. [[CrossRef](#)]
21. Sousa, C.; de Graaf, C.; Rudavskiy, A.; Broer, R.; Tatchen, J.; Etinski, M.; Marian, C.M. Ultrafast deactivation mechanism of the excited singlet in the light-induced spin crossover of $[\text{Fe}(2,2\text{-bipyridine})_3]^{2+}$. *Chem. A Eur. J.* **2013**, *19*, 17541–17551. [[CrossRef](#)]
22. Monat, J.E.; McCusker, J.K. Femtosecond Excited-State Dynamics of an Iron(II) Polypyridyl Solar Cell Sensitizer Model. *J. Am. Chem. Soc.* **2000**, *122*, 4092–4097. [[CrossRef](#)]
23. Engel, N.; Bokarev, S.I.; Moguevski, A.; Raheem, A.A.; Al-Obaidi, R.; Möhle, T.; Grell, G.; Siefermann, K.R.; Abel, B.; Aziz, S.G.; et al. Light-induced relaxation dynamics of the ferricyanide ion revisited by ultrafast XUV photoelectron spectroscopy. *Phys. Chem. Chem. Phys.* **2017**, *19*, 14248–14255. [[CrossRef](#)]
24. Penfold, T.J.; Gindensperger, E.; Daniel, C.; Marian, C.M. Spin-Vibronic Mechanism for Intersystem Crossing. *Chem. Rev.* **2018**, *118*, 6975–7025. [[CrossRef](#)]
25. Alexander, J.J.; Gray, H.B. Electronic Structures of Hexacyanometalate Complexes. *J. Am. Chem. Soc.* **1968**, *90*, 4260–4271. [[CrossRef](#)]
26. *CRC Handbook of Chemistry and Physics*, 100th ed.; Rumble, J.R. (Ed.) CRC Press: Boca Raton, FL, USA; London, UK; New York, NY, USA, 2019.
27. Ponseca, C.S.; Chábera, P.; Uhlig, J.; Persson, P.; Sundström, V. Ultrafast Electron Dynamics in Solar Energy Conversion. *Chem. Rev.* **2017**, *117*, 10940–11024. [[CrossRef](#)]
28. Chen, J.; Browne, W.R. *Photochemistry of Iron Complexes*; Elsevier: Amsterdam, The Netherlands, 2018. [[CrossRef](#)]
29. Vöhringer, P. Vibrations tell the tale. A time-resolved mid-infrared perspective of the photochemistry of iron complexes. *Dalt. Trans.* **2019**, *49*, 256–266. [[CrossRef](#)]
30. Scattergood, P.A.; Sinopoli, A.; Elliott, P.I.P. Photophysics and photochemistry of 1,2,3-triazole-based complexes. *Coord. Chem. Rev.* **2017**, *350*, 136–154. [[CrossRef](#)]
31. Duchanois, T.; Liu, L.; Pastore, M.; Monari, A.; Cebrián, C.; Trolez, Y.; Darari, M.; Magra, K.; Francés-Monerris, A.; Domenichini, E.; et al. NHC-Based Iron Sensitizers for DSSCs. *Inorganics* **2018**, *6*, 63. [[CrossRef](#)]
32. Pastore, M.; Duchanois, T.; Liu, L.; Monari, A.; Assfeld, X.; Haacke, S.; Gros, P.C. Interfacial charge separation and photovoltaic efficiency in Fe(II)-carbene sensitized solar cells. *Phys. Chem. Chem. Phys.* **2016**, *18*, 28069–28081. [[CrossRef](#)]
33. Chabera, P.; Lindh, L.; Rosemann, N.W.; Prakash, O.; Uhlig, J.; Yartsev, A.; Wärnmark, K.; Sundström, V.; Persson, P. Photofunctionality of Iron N-Heterocyclic Carbenes and Related d5 Complexes. *Coord. Chem. Rev.* **2020**. submitted.
34. Kaufhold, S.; Wärnmark, K. Design and synthesis of photoactive iron n-heterocyclic carbene complexes. *Catalysts* **2020**, *10*, 132. [[CrossRef](#)]
35. Hagfeldt, A.; Graetzel, M. Light-Induced Redox Reactions in Nanocrystalline Systems. *Chem. Rev.* **1995**, *95*, 49–68. [[CrossRef](#)]
36. Meyer, G.J. Molecular approaches to solar energy conversion with coordination compounds anchored to semiconductor surfaces. *Inorg. Chem.* **2005**, *44*, 6852–6864. [[CrossRef](#)]
37. Mccusker, J.K. Femtosecond Absorption Spectroscopy of Transition Metal Charge-Transfer Complexes. *Acc. Chem. Res.* **2003**, *36*, 876–887. [[CrossRef](#)]

38. Reinhard, M.; Penfold, T.J.; Lima, F.A.; Rittmann, J.; Rittmann-Frank, M.H.; Abela, R.; Tavernelli, I.; Rothlisberger, U.; Milne, C.J.; Chergui, M. Photooxidation and photoaquation of iron hexacyanide in aqueous solution: A picosecond X-ray absorption study. *Struct. Dyn.* **2014**, *1*. [CrossRef]
39. Chergui, M.; Collet, E. Photoinduced Structural Dynamics of Molecular Systems Mapped by Time-Resolved X-ray Methods. *Chem. Rev.* **2017**, *117*, 11025–11065. [CrossRef]
40. Gütllich, P.; Hauser, A.; Spiering, H. Thermal and Optical Switching of Iron(II) Complexes. *Angew. Chem. Int. Ed. Engl.* **1994**, *33*, 2024–2054. [CrossRef]
41. Decurtins, S.; Gütllich, P.; Hasselbach, K.M.; Hauser, A.; Spiering, H. Light-induced excited-spin-state trapping in iron(II) spin-crossover systems. Optical spectroscopic and magnetic susceptibility study. *Inorg. Chem.* **1985**, *24*, 2174–2178. [CrossRef]
42. Cannizzo, A.; Milne, C.J.; Consani, C.; Gawelda, W.; Bressler, C.; van Mourik, F.; Chergui, M. Light-induced spin crossover in Fe(II)-based complexes: The full photocycle unraveled by ultrafast optical and X-ray spectroscopies. *Coord. Chem. Rev.* **2009**, *254*, 2677–2686. [CrossRef]
43. Mukherjee, S.; Torres, D.E.; Jakubikova, E. HOMO inversion as a strategy for improving the light-absorption properties of Fe(II) chromophores. *Chem. Sci.* **2017**, *8*, 8115–8126. [CrossRef] [PubMed]
44. Fredin, L.A.; Pápai, M.; Rozsályi, E.; Vankó, G.; Wärnmark, K.; Sundström, V.; Persson, P. Exceptional Excited State Lifetime of an Iron (II) N-heterocyclic Carbene Complex Explained. *J. Phys. Chem. Lett.* **2014**, *5*, 2066–2071. [CrossRef] [PubMed]
45. Dixon, I.M.; Alary, F.; Boggio-Pasqua, M.; Heully, J.L. The (N₄C₂)²⁻ donor set as promising motif for bis(tridentate) iron(II) photoactive compounds. *Inorg. Chem.* **2013**, *52*, 13369–13374. [CrossRef] [PubMed]
46. Bowman, D.N.; Bondarev, A.; Mukherjee, S.; Jakubikova, E. Tuning the Electronic Structure of Fe(II) Polypyridines via Donor Atom and Ligand Scaffold Modifications: A Computational Study. *Inorg. Chem.* **2015**, *54*, 8786–8793. [CrossRef] [PubMed]
47. Nance, J.; Bowman, D.N.; Mukherjee, S.; Kelley, C.T.; Jakubikova, E. Insights into the Spin-State Transitions in [Fe(tpy)₂]²⁺: Importance of the Terpyridine Rocking Motion. *Inorg. Chem.* **2015**, *54*, 11259–11268. [CrossRef]
48. Canton, S.E.; Zhang, X.; Daku, M.L.; Smeigh, A.L.; Zhang, J.; Liu, Y.; Wallentin, C.-J.; Attenkofer, K.; Jennings, G.; Kurtz, C.A.; et al. Probing the Anisotropic Distortion of Photoexcited Spin Crossover Complexes with Picosecond X-ray Absorption Spectroscopy. *J. Phys. Chem. C* **2014**, *118*, 4536–4545. [CrossRef]
49. Leshchev, D.; Harlang, T.C.B.; Fredin, L.A.; Khakhulin, D.; Liu, Y.; Biasin, E.; Laursen, M.G.; Newby, G.E.; Haldrup, K.; Nielsen, M.M.; et al. Tracking the picosecond deactivation dynamics of a photoexcited iron carbene complex by time-resolved X-ray scattering. *Chem. Sci.* **2018**, *9*, 405–414. [CrossRef]
50. Ashley, D.C.; Jakubikova, E. Ironing out the photochemical and spin-crossover behavior of Fe(II) coordination compounds with computational chemistry. *Coord. Chem. Rev.* **2017**, *337*, 97–111. [CrossRef]
51. Ingleson, M.J.; Layfield, R.A. N-Heterocyclic carbene chemistry of iron: Fundamentals and applications. *Chem. Commun.* **2012**, *48*, 3579–3589. [CrossRef]
52. Chábera, P.; Liu, Y.; Prakash, O.; Thyrahaug, E.; el Nahhas, A.; Honarfar, A.; Essén, S.; Fredin, L.A.; Harlang, T.C.B.; Kjær, K.S.; et al. A low-spin Fe(III) complex with 100-ps ligand-to-metal charge transfer photoluminescence. *Nature* **2017**, *543*, 695–699. [CrossRef]
53. Kjær, K.S.; Kaul, N.; Prakash, O.; Chábera, P.; Rosemann, N.W.; Honarfar, A.; Gordivska, O.; Fredin, L.A.; Bergquist, K.-E.E.; Häggström, L.; et al. Luminescence and reactivity of a charge-transfer excited iron complex with nanosecond lifetime. *Science* **2019**, *363*, 249–253. [CrossRef]
54. Liu, Y.; Harlang, T.; Canton, S.E.; Chábera, P.; Suárez-Alcántara, K.; Fleckhaus, A.; Vithanage, D.A.; Göransson, E.; Corani, A.; Lomoth, R.; et al. Towards longer-lived metal-to-ligand charge transfer states of iron(II) complexes: An N-heterocyclic carbene approach. *Chem. Commun.* **2013**, *49*, 6412–6414. [CrossRef]
55. Pavlishchuk, V.V.; Addison, A.W. Conversion constants for redox potentials measured versus different reference electrodes in acetonitrile solutions at 25 °C. *Inorganica Chim. Acta.* **2000**, *298*, 97–102. Available online: www.elsevier.nl/locate/ica (accessed on 31 July 2017).
56. Zimmer, P.; Burkhardt, L.; Schepper, R.; Zheng, K.; Gosztola, D.; Neuba, A.; Flörke, U.; Wölper, C.; Schoch, R.; Gawelda, W.; et al. Towards Noble-Metal-Free Dyads: Ground and Excited State Tuning by a Cobalt Dimethylglyoxime Motif Connected to an Iron N-Heterocyclic Carbene Photosensitizer. *Eur. J. Inorg. Chem.* **2018**, *2018*, 5203–5214. [CrossRef]

57. Zimmer, P.; Müller, P.; Burkhardt, L.; Schepper, R.; Neuba, A.; Steube, J.; Dietrich, F.; Flörke, U.; Mangold, S.; Gerhards, M.; et al. N-Heterocyclic Carbene Complexes of Iron as Photosensitizers for Light-Induced Water Reduction. *Eur. J. Inorg. Chem.* **2017**, *2017*, 1504–1509. [[CrossRef](#)]
58. Duchanois, T.; Etienne, T.; Beley, M.; Assfeld, X.; Perpète, E.A.; Monari, A.; Gros, P.C. Heteroleptic pyridyl-carbene iron complexes with tuneable electronic properties. *Eur. J. Inorg. Chem.* **2014**, *2014*, 3747–3753. [[CrossRef](#)]
59. Duchanois, T.; Etienne, T.; Cebrián, C.; Liu, L.; Monari, A.; Beley, M.; Assfeld, X.; Haacke, S.; Gros, P.C. An iron-based photosensitizer with extended excited-state lifetime: Photophysical and photovoltaic properties. *Eur. J. Inorg. Chem.* **2015**, *2015*, 2469–2477. [[CrossRef](#)]
60. Zimmer, P.; Burkhardt, L.; Friedrich, A.; Steube, J.; Neuba, A.; Schepper, R.; Müller, P.; Flörke, U.; Huber, M.; Lochbrunner, S.; et al. The Connection between NHC Ligand Count and Photophysical Properties in Fe(II) Photosensitizers: An Experimental Study. *Inorg. Chem.* **2018**, *57*, 360–373. [[CrossRef](#)]
61. Liu, Y.; Kjaer, K.S.; Fredin, L.A.; Chabera, P.; Harlang, T.; Canton, S.E.; Lidin, S.; Zhang, J.; Lomoth, R.; Bergquist, K.E.; et al. A heteroleptic ferrous complex with mesoionic bis(1,2,3-triazol-5-ylidene) ligands: Taming the MLCT excited state of iron(II). *Chem. A Eur. J.* **2015**, *21*, 3628–3639. [[CrossRef](#)]
62. Liu, L.; Duchanois, T.; Etienne, T.; Monari, A.; Beley, M.; Assfeld, X.; Haacke, S.; Gros, P.C. A new record excited state 3MLCT lifetime for metalorganic iron(II) complexes. *Phys. Chem. Chem. Phys.* **2016**, *18*, 12550–12556. [[CrossRef](#)]
63. Darari, M.; Domenichini, E.; Francés-Monerris, A.; Cebrián, C.; Magra, K.; Beley, M.; Pastore, M.; Monari, A.; Assfeld, X.; Haacke, S.; et al. Iron(ii) complexes with diazanyl-NHC ligands: Impact of π -deficiency of the azine core on photophysical properties. *Dalt. Trans.* **2019**, *48*, 10915–10926. [[CrossRef](#)]
64. Francés-Monerris, A.; Magra, K.; Darari, M.; Cebrián, C.; Beley, M.; Domenichini, E.; Haacke, S.; Pastore, M.; Assfeld, X.; Gros, P.C.; et al. Synthesis and Computational Study of a Pyridylcarbene Fe(II) Complex: Unexpected Effects of fac/mer Isomerism in Metal-to-Ligand Triplet Potential Energy Surfaces. *Inorg. Chem.* **2018**, *57*, 10431–10441. [[CrossRef](#)]
65. Magra, K.; Domenichini, E.; Francés-Monerris, A.; Cebrián, C.; Beley, M.; Darari, M.; Pastore, M.; Monari, A.; Assfeld, X.; Haacke, S.; et al. Impact of the fac/mer Isomerism on the Excited-State Dynamics of Pyridyl-carbene Fe(II) Complexes. *Inorg. Chem.* **2019**, *58*, 5069–5081. [[CrossRef](#)]
66. Chábera, P.; Kjaer, K.S.; Prakash, O.; Honarfar, A.; Liu, Y.; Fredin, L.A.; Harlang, T.C.B.; Lidin, S.; Uhlig, J.; Sundström, V.; et al. FeII Hexa N-Heterocyclic Carbene Complex with a 528 ps Metal-To-Ligand Charge-Transfer Excited-State Lifetime. *J. Phys. Chem. Lett.* **2018**, *9*, 459–463. [[CrossRef](#)]
67. Tatsuno, H.; Kjær, K.S.; Kunnus, K.; Harlang, T.C.B.; Timm, C.; Guo, M.; Chábera, P.; Fredin, L.A.; Hartsock, R.W.; Reinhard, M.E.; et al. Hot Branching Dynamics in a Light-Harvesting Iron Carbene Complex Revealed by Ultrafast X-ray Emission Spectroscopy. *Angew. Chem.* **2020**, *132*, 372–380. [[CrossRef](#)]
68. Kunnus, K.; Vacher, M.; Harlang, T.C.B.; Kjær, K.S.; Haldrup, K.; Biasin, E.; van Driel, T.B.; Pápai, M.; Chabera, P.; Liu, Y.; et al. Origin of vibrational wavepacket dynamics in Fe carbene photosensitizer determined with femtosecond X-ray emission and scattering. *Nat. Commun.* **2020**, *11*, 1–11. [[CrossRef](#)]
69. Pápai, M.; Penfold, T.J.; Møller, K.B. Effect of tert-Butyl Functionalization on the Photoexcited Decay of a Fe(II)-N-Heterocyclic Carbene Complex. *J. Phys. Chem. C* **2016**, *120*, 17234–17241. [[CrossRef](#)]
70. Penfold, T.J.; Pápai, M.; Rozgonyi, T.; Møller, K.B.; Vankó, G. Probing spin-vibronic dynamics using femtosecond X-ray spectroscopy. In *Faraday Discuss*; The Royal Society of Chemistry: London, UK, 2016; pp. 731–746. [[CrossRef](#)]
71. Pápai, M.; Vankó, G.; Rozgonyi, T.; Penfold, T.J. High-Efficiency Iron Photosensitizer Explained with Quantum Wavepacket Dynamics. *J. Phys. Chem. Lett.* **2016**, *7*, 2009–2014. [[CrossRef](#)]
72. Pápai, M.; Simmermacher, M.; Penfold, T.J.; Møller, K.B.; Rozgonyi, T. How to Excite Nuclear Wavepackets into Electronically Degenerate States in Spin-Vibronic Quantum Dynamics Simulations. *J. Chem. Theory Comput.* **2018**, *14*, 3967–3974. [[CrossRef](#)]
73. Pápai, M.; Abedi, M.; Levi, G.; Biasin, E.; Nielsen, M.M.; Møller, K.B. Theoretical Evidence of Solvent-Mediated Excited-State Dynamics in a Functionalized Iron Sensitizer. *J. Phys. Chem. C* **2019**, *123*, 2056–2065. [[CrossRef](#)]
74. Pápai, M.; Rozgonyi, T.; Penfold, T.J.; Nielsen, M.M.; Møller, K.B. Simulation of ultrafast excited-state dynamics and elastic x-ray scattering by quantum wavepacket dynamics. *J. Chem. Phys.* **2019**, *151*, 104307. [[CrossRef](#)]

75. Canton, S.E.; Zhang, X.; Daku, M.L.L.; Liu, Y.; Zhang, J.; Alvarez, S. Mapping the ultrafast changes of continuous shape measures in photoexcited spin crossover complexes without long-range order. *J. Phys. Chem. C* **2015**, *119*, 3322–3330. [[CrossRef](#)]
76. Chábera, P.; Fredin, L.A.; Kjær, K.S.; Rosemann, N.W.; Lindh, L.; Prakash, O.; Liu, Y.; Wärnmark, K.; Uhlig, J.; Sundström, V.; et al. Band-selective dynamics in charge-transfer excited iron carbene complexes. *Faraday Discuss.* **2019**, *216*, 191–210. [[CrossRef](#)]
77. Hagfeldt, A.; Grätzel, M. Molecular photovoltaics. *Acc. Chem. Res.* **2000**, *33*, 269–277. [[CrossRef](#)]
78. Ardo, S.; Meyer, G.J. Photodriven heterogeneous charge transfer with transition-metal compounds anchored to TiO₂ semiconductor surfaces. *Chem. Soc. Rev.* **2009**, *38*, 115–164. [[CrossRef](#)]
79. Grätzel, M. Solar energy conversion by dye-sensitized photovoltaic cells. *Inorg. Chem.* **2005**, *44*, 6841–6851. [[CrossRef](#)]
80. Galoppini, E. Linkers for anchoring sensitizers to semiconductor nanoparticles. *Coord. Chem. Rev.* **2004**, *248*, 1283–1297. [[CrossRef](#)]
81. Ferrere, S.; Gregg, B.A. Photosensitization of TiO₂ by [Fe(II)(2,2'-bipyridine-4,4'-dicarboxylic acid)₂(CN)₂]: Band Selective Electron Injection from Ultra-Short-Lived Excited States. 1993. Available online: <https://pubs.acs.org/sharingguidelines> (accessed on 17 January 2019).
82. Ferrere, S. New photosensitizers based upon [Fe(II)(L)₂(CN)₂] and [Fe(III)L₃], where L is substituted 2,2'-bipyridine. *Inorg. Chim. Acta* **2002**, *329*, 79–92. [[CrossRef](#)]
83. Yang, M.; Thompson, D.W.; Meyer, G.J. Dual Pathways for TiO₂ Sensitization by Na₂[Fe(bpy)(CN)₄]. *Inorg. Chem.* **2000**, *39*, 3738–3739. [[CrossRef](#)]
84. Yang, M.; Thompson, D.W.; Meyer, G.J. Charge-transfer studies of iron cyano compounds bound to nanocrystalline TiO₂ surfaces. *Inorg. Chem.* **2002**, *41*, 1254–1262. [[CrossRef](#)]
85. Harlang, T.C.B.; Liu, Y.; Gordivska, O.; Fredin, L.A.; Ponseca, C.S.; Huang, P.; Chábera, P.; Kjaer, K.S.; Mateos, H.; Uhlig, J.; et al. Iron sensitizer converts light to electrons with 92% yield. *Nat. Chem.* **2015**, *7*, 883–889. [[CrossRef](#)]
86. Fredin, L.A.; Wärnmark, K.; Sundström, V.; Persson, P. Molecular and Interfacial Calculations of Iron(II) Light Harvesters. *ChemSusChem* **2016**, *9*, 667–675. [[CrossRef](#)]
87. Mukherjee, S.; Liu, C.; Jakubikova, E. Comparison of interfacial electron transfer efficiency in [Fe(ctpy)₂]²⁺-TiO₂ and [Fe(cCNC)₂]²⁺-TiO₂ Assemblies: Importance of conformational sampling. *J. Phys. Chem. A* **2018**, *122*, 1821–1830. [[CrossRef](#)]
88. Bowman, D.N.; Mukherjee, S.; Barnes, L.J.; Jakubikova, E. Linker dependence of interfacial electron transfer rates in Fe(II)-polypyridine sensitized solar cells. *J. Phys. Condens. Matter.* **2015**, *27*, 134205. [[CrossRef](#)]
89. Jakubikova, E.; Bowman, D.N. Fe(II)-Polypyridines as Chromophores in Dye-Sensitized Solar Cells: A Computational Perspective. *Acc. Chem. Res.* **2015**, *48*, 1441–1449. [[CrossRef](#)]
90. Karpacheva, M.; Housecroft, C.E.; Constable, E.C. Electrolyte tuning in dye-sensitized solar cells with N-heterocyclic carbene (NHC) iron(II) sensitizers. *Beilstein J. Nanotechnol.* **2018**, *9*, 3069–3078. [[CrossRef](#)]
91. Karpacheva, M.; Wyss, V.; Housecroft, C.E.; Constable, E.C. There Is a Future for N-Heterocyclic Carbene Iron(II) Dyes in Dye-Sensitized Solar Cells: Improving Performance through Changes in the Electrolyte. *Materials* **2019**, *12*, 4181. [[CrossRef](#)]
92. Marchini, E.; Darari, M.; Lazzarin, L.; Boaretto, R.; Argazzi, R.; Bignozzi, C.A.; Gros, P.C.; Caramori, S. Recombination and regeneration dynamics in FeNHC(II)-sensitized solar cells. *Chem. Commun.* **2020**, *56*, 543–546. [[CrossRef](#)]
93. Vogler, A.; Kunkely, H. Charge transfer excitation of organometallic compounds. *Coord. Chem. Rev.* **2004**, *248*, 273–278. [[CrossRef](#)]
94. Fränkel, R.; Kernbach, U.; Bakola-Christianopoulou, M.; Plaia, U.; Suter, M.; Ponikwar, W.; Nöth, H.; Moinet, C.; Fehlhammer, W.P. Homoleptic carbene complexes: Part VIII. Hexacarbene complexes. *J. Organomet. Chem.* **2001**. [[CrossRef](#)]
95. Ericson, F.; Honarfar, A.; Prakash, O.; Tatsuno, H.; Fredin, L.A.; Handrup, K.; Chábera, P.; Gordivska, O.; Kjær, K.S.; Liu, Y.; et al. Electronic structure and excited state properties of iron carbene photosensitizers – A combined X-ray absorption and quantum chemical investigation. *Chem. Phys. Lett.* **2017**, *683*, 559–566. [[CrossRef](#)]

96. Temperton, R.H.; Rosemann, N.W.; Guo, M.; Johansson, N.; Fredin, L.A.; Prakash, O.; Wärnmark, K.; Handrup, K.; Uhlig, J.; Schnadt, J.; et al. Site-Selective Orbital Interactions in an Ultrathin Iron Carbene Photosensitizer Film. *J. Phys. Chem. A* **2020**, *124*, 1603–1609. [CrossRef] [PubMed]
97. Hunter, B.M.; Gray, H.B.; Müller, A.M. Earth-Abundant Heterogeneous Water Oxidation Catalysts. *Chem. Rev.* **2016**, *116*, 14120–14136. [CrossRef] [PubMed]
98. Su, B.; Cao, Z.C.; Shi, Z.J. Exploration of Earth-Abundant Transition Metals (Fe, Co, and Ni) as Catalysts in Unreactive Chemical Bond Activations. *Acc. Chem. Res.* **2015**, *48*, 886–896. [CrossRef]
99. Blakemore, J.D.; Crabtree, R.H.; Brudvig, G.W. Molecular Catalysts for Water Oxidation. *Chem. Rev.* **2015**, *115*, 12974–13005. [CrossRef]
100. Lewis, N.S.; Nocera, D.G. Powering the planet: Chemical challenges in solar energy utilization. *Proc. Natl. Acad. Sci. USA* **2006**, *103*, 15729–15735. [CrossRef]
101. Nocera, D.G. The artificial leaf. *Acc. Chem. Res.* **2012**, *45*, 767–776. [CrossRef]
102. Kärkäs, M.D.; Verho, O.; Johnston, E.V.; Åkermark, B. Artificial photosynthesis: Molecular systems for catalytic water oxidation. *Chem. Rev.* **2014**, *114*, 11863–12001. [CrossRef]
103. Magnusson, A.; Anderlund, M.; Johansson, O.; Lindblad, P.; Lomoth, R.; Polivka, T.; Ott, S.; Stensjo, K.; Styring, S.; Sundstrom, V.; et al. Biomimetic and Microbial Approaches to Solar Fuel Generation. *Acc. Chem. Res.* **2009**, *42*, 1899. [CrossRef]
104. Chen, J.; Browne, W.R. Photochemistry of iron complexes. *Coord. Chem. Rev.* **2018**, *374*, 15–35. [CrossRef]
105. Danforth, R.A.; Kohler, B. Ultrafast photochemical dynamics of the hexaquaquairon(III) ion. *Chem. Phys. Lett.* **2017**, *683*, 315–321. [CrossRef]
106. Pöpcke, A.; Friedrich, A.; Lochbrunner, S. Revealing the initial steps in homogeneous photocatalysis by time-resolved spectroscopy. *J. Phys. Condens. Matter.* **2020**, *32*, 153001. [CrossRef]
107. Smith, J.M. Strongly donating scorpionate ligands. *Comments Inorg. Chem.* **2008**, *29*, 189–233. [CrossRef]
108. Baslon, V.; Harris, J.P.; Reber, C.; Colmer, H.E.; Jackson, T.A.; Forshaw, A.P.; Smith, J.M.; Kinney, R.A.; Telser, J. Near-infrared 2Eg → 4A2g and visible LMCT luminescence from a molecular bis-(tris(carbene)borate) manganese(IV) complex. *Can. J. Chem.* **2017**, *95*, 547–552. [CrossRef]
109. Young, E.R.; Oldacre, A. Iron hits the mark. *Science* **2019**, *363*, 225–226. [CrossRef]
110. Lee, Y.F.; Kirchhoff, J.R. Absorption and Luminescence Spectroelectrochemical Characterization of a Highly Luminescent Rhenium(I) Complex. *J. Am. Chem. Soc.* **1994**, *116*, 3599–3600. [CrossRef]
111. Adams, J.J.; Arulsamy, N.; Sullivan, B.P.; Roddick, D.M.; Neuberger, A.; Schmehl, R.H. Homoleptic Tris-Diphosphine Re(I) and Re(II) Complexes and Re(II) Photophysics and Photochemistry. *Inorg. Chem.* **2015**, *54*, 11136–11149. [CrossRef]
112. Del Negro, A.S.; Seliskar, C.J.; Heineman, W.R.; Hightower, S.E.; Bryan, S.A.; Sullivan, B.P. Highly oxidizing excited states of Re and Tc complexes. *J. Am. Chem. Soc.* **2006**, *128*, 16494–16495. [CrossRef]
113. Francés-Monerris, A.; Gros, P.C.; Pastore, M.; Assfeld, X.; Monari, A. Photophysical properties of bichromophoric Fe(II) complexes bearing an aromatic electron acceptor. *Theor. Chem. Acc.* **2019**, *138*, 86. [CrossRef]
114. Vogler, A.; Kunkely, H. *Luminescent Metal Complexes: Diversity of Excited States*; Yersin, H., Ed.; Top. Curr. Chem. 2013—Transition Metal and Rare Earth Compounds; Springer: Berlin/Heidelberg, Germany, 2001; pp. 143–182.
115. Braun, J.D.; Lozada, I.B.; Kolodziej, C.; Burda, C.; Newman, K.M.E.; van Lierop, J.; Davis, R.L.; Herbert, D.E. Iron(ii) coordination complexes with panchromatic absorption and nanosecond charge-transfer excited state lifetimes. *Nat. Chem.* **2019**, *11*, 1144–1150. [CrossRef]
116. Steube, J.; Burkhardt, L.; Pöpcke, A.; Moll, J.; Zimmer, P.; Schoch, R.; Wölper, C.; Heinze, K.; Lochbrunner, S.; Bauer, M. Excited-State Kinetics of an Air-Stable Cyclometalated Iron(II) Complex. *Chem. A Eur. J.* **2019**, *25*, 11826–11830. [CrossRef]
117. Hockin, B.M.; Li, C.; Robertson, N.; Zysman-Colman, E. Photoredox catalysts based on earth-abundant metal complexes. *Catal. Sci. Technol.* **2019**, *9*, 889–915. [CrossRef]

